

# A strong-coupling analysis of two-dimensional $O(N)$ $\sigma$ models with $N \leq 2$ on square, triangular and honeycomb lattices

Massimo Campostrini, Andrea Pelissetto, Paolo Rossi, and Ettore Vicari  
*Dipartimento di Fisica dell'Università and I.N.F.N., I-56126 Pisa, Italy*

## Abstract

The critical behavior of two-dimensional  $O(N)$   $\sigma$  models with  $N \leq 2$  on the square, triangular, and honeycomb lattices is investigated by an analysis of the strong-coupling expansion of the two-point fundamental Green's function  $G(x)$ , calculated up to 21st order on the square lattice, 15th order on the triangular lattice, and 30th order on the honeycomb lattice.

For  $N < 2$  the critical behavior is of power-law type, and the exponents  $\gamma$  and  $\nu$  extracted from our strong-coupling analysis confirm exact results derived assuming universality with solvable solid-on-solid models.

At  $N = 2$ , i.e., for the 2- $d$  XY model, the results from all lattices considered are consistent with the Kosterlitz-Thouless exponential approach to criticality, characterized by an exponent  $\sigma = \frac{1}{2}$ , and with universality. The value  $\sigma = \frac{1}{2}$  is confirmed within an uncertainty of few per cent. The prediction  $\eta = \frac{1}{4}$  is also roughly verified.

For various values of  $N \leq 2$ , we determine some ratios of amplitudes concerning the two-point function  $G(x)$  in the critical limit of the symmetric phase. This analysis shows that the low-momentum behavior of  $G(x)$  in the critical region is essentially Gaussian at all values of  $N \leq 2$ . New exact results for the long-distance behavior of  $G(x)$  when  $N = 1$  (Ising model in the strong-coupling phase) confirm this statement.

PACS numbers: 75.10 Hk, 05.50.+q, 11.10 Kk, 64.60 Fr.

## I. INTRODUCTION

The strong-coupling expansion is one of the most successful approaches to the study of critical phenomena. Many important results concerning physical models at criticality have been obtained by deducing the asymptotic critical behavior of physical quantities from their strong-coupling series.

We have calculated the two-point Green's function

$$G(x) = \langle \vec{s}_x \cdot \vec{s}_0 \rangle, \quad (1)$$

of two-dimensional  $O(N)$   $\sigma$  models on the square, triangular and honeycomb lattices, respectively up to 21st, 15th, and 30th order in the strong-coupling expansion. Such calculations were performed within the nearest-neighbor lattice formulation, described by the action

$$S = -N\beta \sum_{\text{links}} \vec{s}_{x_l} \cdot \vec{s}_{x_r}, \quad (2)$$

where  $\vec{s}_x$  is a  $N$ -component vector, the sum runs over all the links, and  $x_l, x_r$  indicate the sites at the ends of each link. The comparison of results from strong-coupling series calculated on different lattices offers the possibility of important tests of universality, which, if positive, strongly confirm the reliability of the final results.

A complete presentation of our strong-coupling computations for  $O(N)$   $\sigma$  models in two and three dimensions will be presented in a forthcoming paper. A preliminary report on our calculations can be found in Ref. [1]. On the square lattice our strong-coupling series represent a considerable extension of the 14th order calculations of Ref. [2], performed by means of a linked cluster expansion, which have been re-elaborated and analyzed in Ref. [3]. We also mention recent works where the linked cluster expansion technique has been further developed and calculations of series up to 18th order [4] and 19th order [5] for bulk quantities in  $d = 2, 3, 4$  have been announced.

In this paper we focus on 2-d  $O(N)$   $\sigma$  models with  $N \leq 2$ . The analysis of our strong-coupling series for models with  $N \geq 3$ , i.e., those enjoying asymptotic freedom, is presented in Ref. [6].

Two-dimensional  $O(N)$   $\sigma$  models with  $N < 2$  should present a standard power-law critical behavior, and should be described at criticality by conformal field theories with central charge  $c < 1$ . The most physically relevant models in this range of values of  $N$  are self-avoiding random walk models and Ising models, corresponding respectively to  $N = 0$  and  $N = 1$ . At  $N = -2$  the critical theory has been proven to be Gaussian [7], i.e.,  $\gamma = 1$ ,  $\nu = \frac{1}{2}$ , and  $\eta = 0$ . Assuming universality with solvable solid-on-solid models, exact formulas for the critical exponents in the range  $-2 < N < 2$  have been proposed [8–10], interpolating the critical behaviors at  $N = -2, 0, 1, 2$ . The critical exponents of the magnetic susceptibility  $\gamma$  and correlation length  $\nu$  are conjectured to be

$$\begin{aligned} \gamma &= \frac{3 + a^2}{4a(2 - a)}, \\ \nu &= \frac{1}{4 - 2a}, \end{aligned} \quad (3)$$

where the parameter  $a$  is determined by the equation

$$N = -2 \cos\left(\frac{2\pi}{a}\right) \quad (4)$$

with the constraint  $1 \leq a \leq 2$ . The exponent  $\eta$  can be obtained by the hyperscaling relation  $\gamma = (2 - \eta)\nu$ .

In the limit  $N \rightarrow 2$  formulas (3) yield  $\gamma \rightarrow \infty$  and  $\nu \rightarrow \infty$ , suggesting that at  $N = 2$  the critical pattern should not follow a power-law behavior. The XY spin model in two dimensions, i.e., the  $N = 2$  model, is conjectured to experience a Kosterlitz-Thouless phase transition [11] of infinite order, characterized by a very weak singularity in the free energy and an exponential divergence of the correlation length at a finite  $\beta$ . This model should describe the critical properties of a number of two-dimensional systems, such as thin films of superfluid helium.

According to the Kosterlitz-Thouless (K-T) scenario, the correlation length is expected to behave like

$$\xi \sim \exp\left(\frac{b}{\tau^\sigma}\right) \quad (5)$$

for  $0 < \tau \equiv 1 - \beta/\beta_c \ll 1$ . The value of the exponent is  $\sigma = \frac{1}{2}$  and  $b$  is a non-universal positive constant. At the critical temperature, the asymptotic behavior for  $r \rightarrow \infty$  of the two-point correlation function should be (cfr. e.g. Ref. [12])

$$G(r)_{\text{crit}} \sim \frac{(\ln r)^{2\theta}}{r^\eta} \left[ 1 + O\left(\frac{\ln \ln r}{\ln r}\right) \right], \quad (6)$$

with  $\eta = \frac{1}{4}$  and  $\theta = \frac{1}{16}$ . Near criticality, i.e., for  $0 < \tau \ll 1$ , the behavior of the magnetic susceptibility can be deduced from Eq. (6):

$$\chi \sim \int_0^\xi dr G(r)_{\text{crit}} \sim \xi^{2-\eta} (\ln \xi)^{2\theta} \left[ 1 + O\left(\frac{\ln \ln \xi}{\ln \xi}\right) \right] \sim \xi^{2-\eta} \tau^{-2\sigma\theta} [1 + O(\tau^\sigma \ln \tau)]. \quad (7)$$

In addition, the 2-d XY model is characterized by a line of critical points, starting from  $\beta = \beta_c$  and extending to  $\beta = \infty$ , with  $\eta$  going to zero as  $1/\beta$  for  $\beta \rightarrow \infty$ . At criticality the 2-d XY model should give rise to a conformal field theory with  $c = 1$ .

Numerical studies based on Monte Carlo simulation techniques and high-temperature expansions seem to support the K-T behavior, but a direct accurate verification of all the K-T predictions is still missing. As pointed out in Ref. [13], for  $\beta < \beta_c$  the corrections to the asymptotic behavior (5) should become really negligible only at very large correlation lengths, out of the reach of standard Monte Carlo simulations on today's computers, which allow  $\xi \lesssim 100$  (cfr. Ref. [14], where simulations for correlation lengths up to  $\xi \simeq 70$  were performed on lattices up to  $512^2$ ). Monte Carlo simulations supplemented with finite-size scaling techniques allow to obtain data for larger  $\xi$ . Ref. [15] shows data up to  $\xi \simeq 850$ , which, although consistent with the K-T prediction, do not really exclude a standard power-law behavior.<sup>1</sup>

---

<sup>1</sup>Actually the author of Ref. [15] claims to favor a conventional power behavior to explain some discrepancies in the determination of the critical exponent  $\eta$ .

Finite-size scaling investigations at criticality are required to be very precise in order to pinpoint the logarithm in the two-point Green's function. On the other hand, if this logarithmic correction is neglected, the precise check of the prediction  $\eta = \frac{1}{4}$  at  $\beta_c$  may be quite hard. The relevance of such logarithmic corrections and some of the consequences of neglecting them have been examined in Ref. [17]. Numerical studies by Monte Carlo renormalization-group and finite-size scaling techniques [16,14] seem to favor a lower value of  $\eta$ , which might be caused by the neglected logarithm. The most accurate verification of the K-T critical pattern has been shown in Ref. [13] by numerically matching the renormalization-group trajectory of the dual of the XY model with that of a the body-centered solid-on-solid model, which has been proven to exhibit a K-T transition. The advantage of this strategy is that such a matching occurs much earlier than the onset of the asymptotic regime, where numerical simulations can provide quite accurate results.

The analysis of the strong-coupling series (cfr. e.g. Refs. [18,19], where a few moments of the two-point Green's function were calculated on the square and triangular lattices respectively up to 20th and 14th order for the special value  $N = 2$ ) substantially supports the K-T mechanism, but it does not provide precise estimates for the exponents  $\sigma$ ,  $\eta$ , and  $\theta$ , probably for two reasons: (i) the asymptotic regime in the terms of the series may be set at very large orders; (ii) the logarithmic correction may cause systematic errors in most of the analysis employed.

The computation of strong-coupling series on the honeycomb lattice and the extension of series on the square and triangular lattices motivate a new strong-coupling analysis of the 2-d XY model. We focus on the K-T mechanism, searching for evidences of this phenomenon.

As already shown in Refs. [6,20], the strong-coupling analysis provides quite accurate continuum-limit estimates when applied to dimensionless ratios of universal quantities, even in the case of asymptotically free models, i.e., when the critical point is  $\beta_c = \infty$ . We define some dimensionless ratios of scaling quantities (ratios of amplitudes) which characterize the low momentum behavior of the two-point function  $G(x)$ , and estimate their values in the critical regime by directly analyzing their strong-coupling series. This will allow us to check how close the low momentum critical behavior of  $G(x)$  is to Gaussian behavior.

The paper is organized as follows:

In Sec. II we investigate the critical behavior of 2-d  $O(N)$   $\sigma$  models with  $N \leq 2$  on the square, triangular and honeycomb lattices, extracting the relevant critical parameters by the analysis of the available strong-coupling series. For  $N < 2$  we compare the strong-coupling estimates of the critical exponents with Eqs. (3). For  $N = 2$ , i.e., the 2-d XY model, we verify the predictions of the K-T critical theory. In particular Sec. II A presents the general features of our strong-coupling analysis. Secs. II B, II C, II D and II E contain detailed reports of the derivations of the various results; they are rather technical and can be skipped by readers not interested in the details of the analysis. In Sec. II F the principal results are summarized and some conclusions are drawn.

In Sec. III we evaluate, at criticality, the values of some amplitude ratios concerning the low-momentum behavior of  $G(x)$ . We will present results for the most physically relevant models with  $N \leq 2$ , i.e., those with  $N = 0, 1, 2$ . We also discuss their implications on the low-momentum behavior of  $G(x)$  in the critical region of the symmetric phase.

In Sec. IV some new exact results concerning the asymptotic large-distance behavior of  $G(x)$  for the Ising models on the square, triangular and honeycomb lattices are presented.

In Apps. A, B, and C we present, for  $N = 0, 1, 2$ , the strong-coupling series of some relevant quantities used in this study, respectively for the square, triangular, and honeycomb lattice.

## II. STRONG-COUPING ANALYSIS OF THE CRITICAL BEHAVIOR

### A. Analysis of the series

From the Green's function  $G(x)$  one can derive many interesting quantities. Defining the moments of  $G(x)$

$$m_{2j} = \sum_x (x^2)^j G(x), \quad (8)$$

we computed on each lattice the magnetic susceptibility  $\chi$ , and the second moment correlation length  $\xi_G^2$ ,

$$\begin{aligned} \chi &\equiv m_0, \\ \xi_G^2 &\equiv \frac{m_2}{4\chi}. \end{aligned} \quad (9)$$

Models with  $N < 2$  should have a power-law critical behavior, which may be appropriately investigated by analyzing the strong-coupling series of  $\chi$  and  $\xi_G^2$ , in order to extract the critical exponents  $\gamma$  and  $\nu$ . For  $N = 2$ , in order to check the exponential approach to criticality predicted by the K-T mechanism and extract the relevant exponent  $\sigma$ , as in Ref. [18], we consider the strong-coupling series of the logarithm of  $\chi$  and  $\xi_G$ . More precisely, since  $\chi = 1 + O(\beta)$  and  $\xi_G^2 = \frac{1}{4}c\beta + O(\beta^2)$ , where  $c$  is the coordination number of the lattice ( $c = 4, 6, 3$  respectively for the square, triangular and honeycomb lattice), we consider the series

$$\begin{aligned} l_\chi &\equiv \beta^{-1} \ln \chi = \sum_{i=0}^{\infty} c_i \beta^i, \\ l_\xi &\equiv \beta^{-1} \ln \left( \frac{4\xi_G^2}{c\beta} \right) = \sum_{i=0}^{\infty} d_i \beta^i. \end{aligned} \quad (10)$$

According to Eqs. (5) and (7)  $l_\chi$  and  $l_\xi$  should behave as

$$l_\chi \sim l_\xi \sim \tau^{-\sigma}, \quad (11)$$

and are therefore suitable for a standard analysis by Padé or integral approximants. A vanishing exponent  $\sigma$  would indicate a standard power-law critical behavior. Conversely a stable non-zero value of  $\sigma$  would exclude a power-law behavior.

Estimates of the critical exponents can be obtained by employing the so-called critical point renormalization method (CPRM) [21]. The idea is that, when

$$\begin{aligned} A(x) &= \sum_i a_i x^i \sim (x_0 - x)^{-\alpha} \\ B(x) &= \sum_i b_i x^i \sim (x_0 - x)^{-\beta}, \end{aligned} \quad (12)$$

we have

$$C(x) = \sum_i \frac{b_i}{a_i} x^i \sim (1-x)^{-(1+\beta-\alpha)}, \quad (13)$$

where now the position of the singularity is known. Therefore the analysis of the series  $C$  may provide an unbiased estimate for the difference between the critical exponents of the two functions  $A$  and  $B$ . In particular this idea can be applied to the case  $B = A^2$ , allowing one to get a direct estimate of the critical exponent of  $A$ , provided a sufficiently large number of terms is known. The reliability of the determination of the critical exponent by this method may be checked by comparing the results for the critical point of an unbiased analysis with the exact result  $x_c = 1$ .

A general technique to extract physical information from a  $n$ th order strong-coupling series  $S(x) = \sum_{i=0}^n c_i x^i$  is constructing approximants  $A(x)$  such that

$$A(x) - S(x) = O(x^{n+1}), \quad (14)$$

and studying their singularities. For a review on the resummation techniques cfr. Ref. [22].  $[l/m]$  Padé approximants (PA's) are ratios of two polynomials of degree  $l$  and  $m$  respectively, such that their Taylor expansion is equal to  $S(x)$  up to  $O(x^{l+m})$ . PA's are expected to converge well to meromorphic analytic functions. More flexibility is achieved by constructing PA's of the logarithmic derivative of  $S(x)$  (Dlog-PA analysis), and therefore enlarging the class of functions which can be reproduced to those having singularities of the form  $(z-z_0)^\gamma$ .  $[l/m]$  Dlog-PA's are obtained by integrating the  $[l/m]$  PA's of the logarithmic derivative of  $S(x)$ . Then a  $[l/m]$  PA uses  $n = l + m$  terms of the series, while a  $[l/m]$  Dlog-PA requires  $n = l + m + 1$  terms.

Other kind of approximants can be constructed as solutions of differential equations [23]. We consider integral approximants (IA's) obtained from a first order linear differential equation

$$Q_m(x)f'(x) + P_l(x)f(x) + R_k(x) = O\left(x^{k+l+m+2}\right), \quad (15)$$

where  $Q_m(x)$ ,  $P_l(x)$  and  $R_k(x)$  are polynomials of order  $m$ ,  $l$ , and  $k$  respectively, and we fix  $Q_m(0) = 1$ . These approximants are singular at the zeroes  $x_0$  of  $Q_m(x)$ , and behave as

$$A(x)|x - x_0|^{-\gamma} + B(x), \quad (16)$$

where  $A(x)$  and  $B(x)$  are regular in the neighborhood of  $x_0$ , and

$$\gamma = -\frac{P_l(x_0)}{Q'_m(x_0)}. \quad (17)$$

When we analyze a  $n$ th order series,  $m$ ,  $l$  and  $k$  must satisfy the condition  $k + l + m + 2 \leq n$ . If the position of the singularity  $x_0$  is known, such an analysis can be easily modified forcing the approximant to have a singularity at  $x_0$  by substituting  $Q_m(x) \rightarrow (1 - x/x_0)\bar{Q}_m(x)$ , where  $\bar{Q}_m(x)$  is still a polynomial of order  $m$  with  $\bar{Q}_m(0) = 1$ .

Unlike Dlog-PA's, IA's are suited to take into account subdominant terms in the vicinity of singularities, thus reducing possible systematic errors in the resummation of the series.

On the other hand, in order to get stable and therefore acceptable results, IA's require in general more terms in the series to be resummed than PA's or Dlog-PA's.

As a final estimate from each analysis we took the average of the results from quasi-diagonal (non-defective) approximants (PA's or IA's) using all available terms of the series. The errors we display are just indicative, and should give an idea of the spread of the results coming from the various approximants which can be constructed from the series at hand. They are the square root of the variance around the estimate of the results coming also from quasi-diagonal approximants constructed from shorter series by one and two terms. In the following we will specify the approximants considered in each analysis. This procedure does not always provide a reliable estimate of the systematic error, which may be underestimated especially when the structure of the function cannot be well reproduced by the class of approximants used. A more reliable estimate of the true uncertainty should come from the comparison of results of different analysis of the same series, and from the analyses of series of different estimators of the same quantity, which in general are not expected to have the same analytic structure.

## B. Critical behavior of models with $-2 < N < 2$

In order to determine the critical exponents  $\gamma$  and  $\nu$  of 2-d  $O(N)$   $\sigma$  models with  $N < 2$ , we analyze the strong-coupling series of  $\chi$  and  $\xi_G^2$  on square (21st order), triangular (15th order) and honeycomb (30th order) lattices. For such models, an analysis of the 14<sup>th</sup> order strong-coupling series on the square lattice, calculated in Ref. [2], has been done in Ref. [3].

For  $N = 0$  (the self-avoiding walk), longer series are available [24,25]. To compare with the literature, observe that we have [26]

$$G(x) = \sum_l \beta^l c_l(x), \quad (18)$$

where  $c_l(x)$  is the number of self-avoiding walks of length  $l$  going from 0 to  $x$ . Therefore  $\chi = \sum_l \beta^l c_l$ , and

$$\chi \xi_G^2 = \frac{1}{4} \sum_l \beta^l c_l \langle R_e^2 \rangle_l, \quad (19)$$

where  $c_l = \sum_x c_l(x)$  is the total number of self-avoiding walk of length  $l$  starting from the origin, and

$$\langle R_e^2 \rangle_l = \frac{1}{c_l} \sum_x x^2 c_l(x) \quad (20)$$

is called the “mean end-to-end distance” in self-avoiding walks literature.

Table I shows the results of a Dlog-PA analysis, reporting, for various values of  $N$  and for each lattice,  $\beta_c^{(\chi)}$  and  $\gamma$  as obtained from the strong-coupling series of  $\chi$ , and  $\beta_c^{(\xi)}$  and  $\nu$  from that of  $\xi_G^2$ . Differences between  $\beta_c^{(\chi)}$  and  $\beta_c^{(\xi)}$  should give an idea of the real uncertainty on  $\beta_c$ . In the analysis of  $\chi$  we considered Dlog-PA's with  $l + m \geq 18$  and  $m \geq l \geq 8$  on the square lattice,  $l + m \geq 12$  and  $m \geq l \geq 5$  on the triangular lattice,  $l + m \geq 27$  and

$m \geq l \geq 12$  on the honeycomb lattice. In the analysis of  $\beta^{-1}\xi_G^2$  we considered Dlog-PA's with  $l+m \geq 17$  and  $m \geq l \geq 8$  on the square lattice,  $l+m \geq 11$  and  $m \geq l \geq 5$  on the triangular lattice,  $l+m \geq 26$  and  $m \geq l \geq 12$  on the honeycomb lattice. We tried also IA's, obtaining consistent results, which however only in few cases turned out to be more precise than those of the Dlog-PA's, so we do not report them. For sake of completeness and also to give an idea of the precision we can achieve with such an analysis, in Table I we report also results for  $N = 0, 1$  as obtained from our series, although exact results independent of the conjecture (3) exist for such values of  $N$ . We warn that the errors displayed in Table I are related to the spread of the results from the Dlog-PA's considered, according to the procedure described in the Sec. II A, and therefore they are not always reliable estimates of the uncertainty.

In the range  $-1 \lesssim N \lesssim \frac{3}{2}$  the formulas (3) for the exponents  $\gamma$  and  $\nu$  are well reproduced, and universality is verified. Less precise determinations are obtained when approaching the endpoints  $N = \pm 2$ , presumably due to a rather slow convergence of the corresponding series to their asymptotic regime.

We note that for models with  $N \gtrsim 1$  on the honeycomb lattice the physical critical point is not the singularity closest to the origin, but there is a pair of closer singularities on the imaginary axis. For instance, in the Ising model the physical singularity is placed at  $\beta_c = \frac{1}{2}(2 + \sqrt{3}) = 0.658478\dots$  and there is a pair of singularities at  $\bar{\beta} = \pm i\pi/6$  [27]. Nevertheless Dlog-PA's of the magnetic susceptibility reproduce the physical singularity very precisely: the [15/15] Dlog-PA gives  $\beta_c = 0.658480$  and  $\gamma = 1.74993$ , to be compared with the exact result  $\gamma = \frac{7}{4}$ . The unphysical singularities can be mapped away from the origin by performing the change of variable  $\beta \rightarrow z = \tanh\beta$ , where  $z$  is the character coefficient of the fundamental representation. With decreasing  $N$ ,  $\beta_c$  decreases while the above-mentioned imaginary singularities move away, so that at  $N \lesssim 0$ , the singularity closest to the origin is on the real axis, i.e., it is the physical critical point.

For later comparison with the strong-coupling analysis of 2- $d$  XY model, we have also analyzed the series of  $l_\chi$ , defined in Eq. (10), for the Ising model on the square lattice. Since the critical behavior is of power-law type,  $l_\chi$  should have a logarithmic singularity at  $\beta_c$ , and therefore an analysis like IA should give  $\sigma \simeq 0$  [23]. Indeed most of the IA's of the 20th order series of  $l_\chi$  give  $|\sigma| \lesssim 0.02$ . We mention that a Dlog-PA analysis leads to misleading results in this case, since in order to reproduce the logarithmic behavior it gives rise to spurious singularities, which make the estimate of  $\sigma$  at  $\beta_c$  unreliable.

### C. The 2- $d$ XY model on the square lattice

On the square lattice a strong-coupling analysis of the lowest moments of  $G(x)$  evaluated up to 20th order can be found in Ref. [18]. Having achieved further extension by one term of such series, we update here the situation on the square lattice. We note that the series obtained from our calculations (some of them are reported in App. A) present small discrepancies with those reported in Ref. [18]: they are in agreement up to 16th order,

but slight different at higher order<sup>2</sup>. We are confident that our series are exact, since they were generated for arbitrary  $N$  and we have checked their  $N \rightarrow \infty$  limit against the exact solution, and compared them with the existing series for  $N = 0, 1$ .

We analyzed the 20th order series of  $l_\chi \equiv \beta^{-1} \ln \chi$  by both Dlog-PA's and IA's. We found  $\beta_c = 0.560(2)$  and  $\sigma = 0.53(4)$  from Dlog-PA's (with  $l+m \geq 18$  and  $m \geq l \geq 7$ ). The integral approximant analysis, whose details are given in Table II, leads to  $\beta_c = 0.558(2)$  and  $\sigma = 0.49(8)$  (considering IA's with  $m+l+k \geq 19$  and  $m \geq l, k \geq 5$ ).

From the strong-coupling series of  $l_\chi$  and  $l_\chi^2$ , we have constructed a new series  $\lambda_\chi$  according to CPRM, and analyzed it by standard methods: Dlog-PA's and IA's. We obtained  $\sigma = 0.51(4)$  by Dlog-PA's (with  $l+m \geq 18$  and  $m \geq l \geq 8$ ) biased by imposing the presence of a singularity at  $x_c = 1$ , and  $\sigma = 0.50(2)$  by biased IA's (with  $m+l+k \geq 16$  and  $m \geq l, k \geq 5$ ). Table III shows some details of the IA analysis of the series of  $\lambda_\chi$ . From unbiased Dlog-PA's and IA's  $x_c$  is found to be equal to one within a few per mille, assuring us on the reliability of the estimates of the exponent  $\sigma$  by this method.

The above unbiased analyses strongly support the K-T prediction (7). Although the estimate of  $\sigma$  does not yet reach the high level of precision which is usually found in the analysis of strong-coupling series of considerable length, we can safely conclude that the value  $\sigma = \frac{1}{2}$  is well verified with an uncertainty of less than 10% on the square lattice.

Unbiased approximants of  $l_\xi$  give less stable but definitely consistent results: we found  $\sigma = 0.59(6)$  from CPRM, i.e., from an IA analysis biased at  $x_c = 1$  (with  $m+l+k \geq 15$  and  $m, l, k \geq 5$ ) of the series  $\lambda_\xi$  constructed from  $l_\xi$  and  $l_\xi^2$  according to CPRM. On the other hand by applying CPRM to the two series  $l_\chi$  and  $l_\xi$  one may verify that  $\sigma_\chi = \sigma_\xi$ . From an IA analysis biasing  $x_c = 1$  (with  $m+l+k \geq 15$  and  $m, l, k \geq 5$ ) we found  $\sigma_\chi - \sigma_\xi = 0.010(6)$ , which represents a good check of Eq. (11).

Once  $\sigma = \frac{1}{2}$  was reasonably verified, we performed a set of biased analysis fixing  $\sigma = \frac{1}{2}$  in order to determine the critical point. A way to bias the value of the exponent at  $\sigma = \frac{1}{2}$  is to analyze the series of the square of  $l_\chi$  and  $l_\xi$  by PA's. By doing so we obtained  $\beta_c = 0.5579(3)$  from  $l_\chi^2$ , and  $\beta_c = 0.558(1)$  from  $l_\xi^2$  (we used PA's with  $l+m \geq 17$  and  $m \geq l \geq 8$ ). Still biasing  $\sigma = \frac{1}{2}$ , IA's yield  $\beta_c = 0.5583(2)$  from  $l_\chi$ , and  $\beta_c = 0.559(1)$  from  $l_\xi$  (here we determine, in a IA analysis biasing the position of the singularity, the value of  $\beta_c$  which produces the exponent  $\sigma = \frac{1}{2}$ .)

No complex singularities closer to the origin than  $\beta_c$  are detected in the various strong-coupling analysis, thus indicating that  $\beta_c$  is also the convergence radius of the strong-coupling expansion.

For  $\beta < \beta_c$  we have compared  $\chi$  and  $\xi_G$  as obtained from our strong-coupling analysis with numerical data, available in the literature up to  $\beta = 1/1.96 = 0.5102\dots$  (corresponding to a correlation length  $\xi \simeq 70$ ) by using standard Monte Carlo simulations [14], and up to  $\beta = 1/1.87 = 0.5347\dots$  by employing also finite-size scaling techniques [15]. Actually most of the Monte Carlo data of  $\xi$  reported in Ref. [14] concern  $\xi_{\text{exp}}$ , i.e., the correlation length extracted from the long distance exponential behavior of  $G(x)$ , but as we shall see in the next section  $\xi_G/\xi_{\text{exp}} \simeq 0.999$  at criticality. In order to get strong-coupling curves of  $\chi$  and

---

<sup>2</sup>The difference is however small, at most  $10^{-6}$ , and it does not change the conclusion of Ref. [18].

$\xi_G$  as functions of  $\beta$ , we used approximants constructed biasing  $\sigma = \frac{1}{2}$ , i.e., PA's of  $l_\chi^2$  and  $l_\xi^2$ , and IA's of  $l_\chi$  and  $l_\xi$  biasing  $\sigma = \frac{1}{2}$ . Fig. 1 compares strong-coupling curves of  $\ln \chi$  with the available Monte Carlo data. Table V reports estimates of  $\xi_G$  by strong-coupling expansion and Monte Carlo simulations for various values of  $\beta$ . The agreement among the different calculations is satisfactory.

In order to determine the exponent  $\eta$  without biasing  $\sigma$ , we considered various quantities which can be constructed using the lowest moments of the two-point Green's function:

$$A_\eta \equiv \frac{l_\chi}{l_\xi} = \frac{1}{2}(1 - \eta) + O(\tau^\sigma \ln \tau), \quad (21)$$

$$B_\eta \equiv (\beta l_\chi)^{-1} \ln \left( 1 + \frac{m_2}{\chi^2} \right) = \frac{\eta}{2 - \eta} + O(\tau^\sigma \ln \tau), \quad (22)$$

$$C_\eta \equiv (\beta l_\xi)^{-1} \ln \left( \frac{m_2}{4\beta\chi^2} \right) = \frac{\eta}{2} + O(\tau^\sigma \ln \tau). \quad (23)$$

An estimate of  $\eta$  may then be obtained by resumming the corresponding strong-coupling series by PA's and Dlog-PA's and evaluating them at  $\beta_c$ . Since all of the above quantities are equally good estimators of the exponent  $\eta$ , differences in the results of their analysis should give an idea of the systematic error in the procedure.

PA's and Dlog-PA's of  $A_\eta$  (with  $l + m \geq 16$  and  $m \geq l \geq 7$ ) lead to quite stable results:  $\eta = 0.228(2)$  (where the error displayed, beside the spread of different approximants, takes into account the uncertainty on  $\beta_c$ ). Similarly we found  $\eta = 0.270(5)$  and  $\eta = 0.226(5)$  respectively from PA's and Dlog-PA's of  $B_\eta$  (with  $l + m \geq 17$  and  $m \geq l \geq 8$ ) and of  $\beta^{-1}C_\eta$  (with  $l + m \geq 15$  and  $m \geq l \geq 7$ ). The differences in such determinations indicate a systematic error of about 10%, and within 10% all results are consistent with the K-T prediction  $\eta = \frac{1}{4}$ . Furthermore, when analyzing the energy-series of  $A_\eta$  (by performing the change of variable  $\beta \rightarrow E$  and evaluating the corresponding approximants at  $E_c \simeq 0.722$ , i.e., the energy value at  $\beta_c \simeq 0.559$  [14]), we obtained again a rather stable result but  $\eta = 0.207(5)$ , confirming the presence of a systematic error of about 10%.

A source of systematic error in this analysis is the  $O(\tau^\sigma \ln \tau)$  correction expected in Eqs. (21), (22) and (23) which cannot be reproduced by PA's and Dlog-PA's. In particular Eq. (21) implies a behavior

$$\text{Dlog}A_\eta \sim \tau^{\sigma-1} \quad (24)$$

in the proximity of to  $\beta_c$ . In the Dlog-PA's the above singularities should be mimicked by a pole shifted at a  $\beta$  larger than  $\beta_c$ . Indeed in the analysis of the series of  $A_\eta$  we have found a singularity typically at  $\beta \simeq 1.1 \div 1.2\beta_c$ . This fact will eventually affect the determination of  $A_\eta$  close to  $\beta_c$  by a systematic error. However, since the singularity is integrable, the error must be finite, and the analysis shows that such errors are actually reasonably small. The behavior (21), neglecting the logarithm, could be reproduced by IA's, but we did not obtain sufficiently stable and therefore acceptable results by them. As a further check we

also performed a biased Dlog-PA analysis of the series of the quantity  $A_\eta - \frac{1}{2}(1 - \eta) \sim \tau^\sigma$  (neglecting logarithmic corrections). By fixing  $\eta = \frac{1}{4}$  and  $\beta_c = 0.559$  we found an exponent  $\sigma \simeq 0.6$ , which is satisfactorily close to the expected value  $\sigma = \frac{1}{2}$ .

The exponent  $\theta$  defined in Eqs. (6) and (7) may be extracted by the analysis of the series of the ratios  $\chi/\xi_G^{2-\eta}$  and  $m_4/\xi_G^{6-\eta}$ , indeed

$$\frac{\chi}{\xi_G^{2-\eta}} \sim \frac{m_4}{\xi_G^{6-\eta}} \sim \tau^{-2\sigma\theta} [1 + O(\tau^\sigma \ln \tau)]. \quad (25)$$

Fixing  $\eta = \frac{1}{4}$ , we performed biased analyses of the 20th order strong coupling series of the above ratios imposing  $\beta_c = 0.559$ . Dlog-PA's (with  $l + m \geq 17$  and  $m, l \geq 8$ ) provide the following estimates for  $\theta$  (obtained taking  $\sigma = \frac{1}{2}$ ):  $\theta = -0.042(5)$  from  $\chi/\xi_G^{2-\eta}$ , and  $\theta = -0.05(2)$  from  $m_4/\xi_G^{6-\eta}$ , where errors take into account, beside the spread of the Dlog-PA results, also the uncertainty on  $\beta_c$ . These numbers, although they confirm the fact that  $|\theta|$  is small, are rather different from the K-T prediction  $\theta = \frac{1}{16}$ . As already mentioned above, a source of systematic error for a Dlog-PA analysis is the correction  $O(\tau^{1/2} \ln \tau)$  to the leading  $\tau^{-\theta}$  behavior in formula (25). Since  $\theta$  is very small, this could cause a relevant departure from its true value. The analysis by IA's biased at  $\beta_c \simeq 0.559$  of the strong coupling series of the ratio  $\chi/\xi_G^{2-\eta}$  does not provide sufficiently stable results for  $\theta$ .

#### D. The 2-d XY model on the triangular lattice

On the triangular lattice strong-coupling series of some lowest moments of  $G(x)$  have been calculated in Ref. [19] up to 14th order. We calculated  $G(x)$  up to 15th order, thus extending by one order earlier calculations. We must again mention the existence of discrepancies between our calculations (cfr. App. B) and those of Ref. [19] in the 14th order terms (again of the order of  $10^{-6}$ ).

We performed on the triangular lattice the kind of analysis presented in the previous Subsection for the square lattice. We analyzed the 14th order series of  $l_\chi \equiv \beta^{-1} \ln \chi$  by both Dlog-PA's and IA's. We found  $\beta_c = 0.3413(3)$ ,  $\sigma = 0.52(2)$  from Dlog-PA's (with  $l + m \geq 11$  and  $m \geq l \geq 5$ ), and  $\beta_c = 0.33986(4)$ ,  $\sigma = 0.473(3)$  from IA's with  $m + l + k \geq 12$  and  $m \geq l, k \geq 3$  (the apparent stability of these IA determinations should not be taken seriously, we remind again that what it is really important for estimating the uncertainty is the comparison of results from different analysis).

The CPRM applied to the strong-coupling series of  $l_\chi$  and  $l_\chi^2$  gives  $\sigma = 0.53(1)$  by biased Dlog-PA's having a singularity fixed at  $x_c = 1$  (with  $l + m \geq 12$  and  $m \geq l \geq 5$ ) and  $\sigma = 0.50(2)$  by biased IA's (with  $m + l + k \geq 11$  and  $m \geq l, k \geq 3$ ). Table IV shows some details of the IA analysis. From unbiased Dlog-PA's and IA's,  $x_c$  is found to be equal to one within a few per mille, assuring us on the reliability of the estimates of the exponent  $\sigma$  by this method.

The critical point renormalization method gives good results also when applied to the series of  $l_\xi$ , leading to  $\sigma = 0.52(4)$ . By applying CPRM to the two series  $l_\chi$  and  $l_\xi$  one finds  $\sigma_\chi - \sigma_\xi = 0.001(2)$  from an IA analysis biased at  $x_c = 1$  (with  $m + l + k \geq 12$  and  $m \geq l, k \geq 3$ ).

We can conclude that the K-T prediction  $\sigma = \frac{1}{2}$  is strongly supported by the above results.

We also performed a set of biased analysis fixing  $\sigma = \frac{1}{2}$  in order to determine the critical point. By analyzing  $l_\chi^2$  and  $l_\xi^2$  by PA's, we obtained  $\beta_c = 0.3400(2)$  and  $\beta_c = 0.3393(1)$  respectively (from PA's with  $l + m \geq 12$  and  $m \geq l \geq 5$ ). IA's of  $l_\xi$  biased at  $\sigma = \frac{1}{2}$  yield  $\beta_c = 0.3410(5)$ , while when applied to  $l_\chi$  such analysis does not lead to relevant results, since it gives rise to spurious singularities in the real axis. A  $\sigma = \frac{1}{2}$  biased estimate of the critical point is then  $\beta_c = 0.340(1)$ .

We obtained estimates of  $\eta$  by resumming the series of  $A_\eta$  and  $B_\eta$  (cfr. Eqs. (21) and (22)) by PA's and Dlog-PA's and evaluating them at  $\beta_c \simeq 0.340$ . PA's and Dlog-PA's of  $A_\eta$  (with  $l + m \geq 10$  and  $m \geq l \geq 5$ ) and of  $B_\eta$  (with  $l + m \geq 11$  and  $m \geq l \geq 5$ ) lead again to quite stable but slightly discrepant results: respectively  $\eta = 0.221(2)$  and  $\eta = 0.270(4)$ . The causes of possible systematic errors in the determination of  $\eta$  are the same as for the square lattice, and we refer to Subs. II C for a discussion.

The analysis of the 14th order strong coupling series of  $\chi/\xi_G^{2-\eta} \sim \tau^{-\theta}$  biased by  $\beta_c \simeq 0.340$  (using Dlog-PA's with  $l + m \geq 11$  and  $l, m \geq 5$ ) yields the estimate  $\theta = -0.045(3)$ , which is consistent with the square lattice result, but not with the K-T prediction. IA's does not provide sufficiently stable results also in this case.

## E. The 2-d XY model on the honeycomb lattice

On the honeycomb lattice we calculated series longer than on the square lattice, up to 30th order. Here the possibility of reaching larger orders is related to the smaller coordination number. However longer series do not necessarily mean that more precise results can be obtained from their analysis. This possibility is related to the approach to the asymptotic regime of the series, which is expected to be set later on lattice with smaller coordination number. Actually, as we shall see, the 30th order series on the honeycomb lattice provide results consistent with the K-T theory and universality, but less precise than those obtained from the series on the square and triangular lattices.

Unbiased analyses of the series for  $l_\chi$  lead to:  $\beta_c = 0.884(1)$  and  $\sigma = 0.55(1)$  from Dlog-PA's (with  $l + m \geq 27$  and  $m \geq l \geq 12$ ), and  $\beta_c = 0.877(6)$ ,  $\sigma = 0.4(2)$  from IA's (with  $m + l + k \geq 27$  and  $m \geq l, k \geq 8$ ). The stability of Dlog-PA's is suspect in this case, indeed we found that, just by adding to the series a simple constant of the order of unity, the change in the estimate of  $\sigma$  turns out to be much larger than the error evaluated from the spread of the estimates of different approximants of the same series. Unlike PA's and IA's, the critical parameters provided by Dlog-PA's do not remain strictly invariant by adding a simple constant; this is only an asymptotic property of the Dlog-PA analysis. An analysis based on CPRM method fails to give stable results in this cases, probably because the available series are not sufficiently long to have their asymptotic regime set.

More stable results are obtained when biasing the exponent at  $\sigma = \frac{1}{2}$ . A check of consistency would be requiring that the critical points as extracted from  $l_\chi$  and  $l_\xi$  are the same. We obtained  $\beta_c = 0.879(1)$  from PA's (with  $l + m \geq 26$  and  $m \geq l \geq 13$ ) of  $l_\chi^2$ , and  $\beta_c = 0.878(2)$  from PA's of  $l_\xi^2$ , which is satisfactory.

It is worth noticing that, unlike what happens on the square and triangular lattices,

on the honeycomb lattice the real singularity corresponding to the critical behavior of the theory is not the singularity closest to the origin in the complex  $\beta$ -plane. A pair of imaginary singularities at  $\beta \simeq \pm i0.482$  is detected in the analysis of the strong-coupling series of  $\chi$ .

Taking as an estimate of the critical point  $\beta_c \simeq 0.880$ , we evaluated  $\eta$  from the series of  $A_\eta$  and  $B_\eta$  defined in Eqs. (21) and (22). Again the value obtained from  $A_\eta$  is about 10% lower than  $\frac{1}{4}$ :  $\eta = 0.231(3)$  (from PA's and Dlog-PA's with  $l+m \geq 26$  and  $m \geq l \geq 11$ ), and that from  $B_\eta$  is about 10% higher:  $\eta = 0.28(1)$  (from PA's and Dlog-PA's with  $l+m \geq 27$  and  $m \geq l \geq 12$ ). The behavior of the estimates from  $A_\eta$  and  $B_\eta$  observed in the various lattice seems to indicate that the source of systematic error is in a sense universal, i.e., it essentially depends on the quantity considered and approximately independent of the lattice.

We again estimated the exponent  $\theta$  from the 29th order strong coupling series of the  $\chi/\xi_G^{2-\eta}$ . Dlog-PA's (with  $l+m \geq 26$  and  $l, m \geq 13$ ) biased at  $\beta_c \simeq 0.880$  give  $\theta = -0.042(6)$ , which is consistent with the estimates from the other lattices.

## F. Conclusions

We have studied the critical properties of 2-d  $O(N)$   $\sigma$  models with  $N \leq 2$  on the square, triangular and honeycomb lattices, by analyzing the strong-coupling expansion of the lowest moments of the two-point fundamental Green's function.

The analysis of the strong-coupling series of  $\chi$  and  $\xi_G^2$  on the square, triangular and honeycomb lattices has substantially confirmed that models with  $N < 2$  present a standard power-law critical behavior with critical exponents given by Eqs. (3). We obtained rather precise determinations of the critical exponents in the region  $-1 \lesssim N \lesssim \frac{3}{2}$  (cfr. Table I), where formulas (3) are verified within 1%. The strong-coupling analysis becomes less precise approaching the endpoints  $N = \pm 2$ , presumably due to a rather slow convergence of the corresponding series to their asymptotic regime. Universality among models on the square, triangular and honeycomb lattices has been verified.

The determinations of  $\beta_c$  and  $\sigma$  for the 2-d XY model on the three different lattices are summarized in Table VI. These results are consistent with the K-T exponential approach to criticality and with universality. The best estimates of  $\sigma$  come from the analysis of the series of the magnetic susceptibility, leading to a confirm of the value  $\sigma = \frac{1}{2}$  within an uncertainty of few per cent. The analysis of the series of the correlation length  $\xi_G^2$  yields consistent results. The critical point renormalization method [21] provides the most precise unbiased estimates of  $\sigma$  on the square and triangular lattices. These results rule out the possibility of a standard power-law critical behavior.

On the square lattice most estimates of  $\beta_c$  yielded by our analyses lie in the range  $0.558 \leq \beta_c \leq 0.560$ , although the lowest value  $\beta_c = 0.558$  seems to be favored. This value is consistent with the results of an exponential fit to data of  $\xi$  up to  $\xi \simeq 850$  [15], which yielded  $\beta_c = 0.5593(13)$  and  $\sigma = 0.46(3)$ , and with a biased exponential fit fixing  $\sigma = \frac{1}{2}$  to data up to  $\xi \simeq 70$  produced by a standard Monte Carlo simulations [14], which gave  $\beta_c = 0.559(3)$ . But it is slightly smaller than the quite precise Monte Carlo renormalization group determination of Ref. [13]:  $\beta_c = 0.55985(25)$ . The comparison of (suitable) resummations of the strong-coupling series of  $\chi$  and  $\xi_G^2$  with Monte Carlo data (available up to  $\xi \simeq 850$ ) turns out to be quite satisfactory (cfr. Table V), giving further support to our conclusions.

The prediction  $\eta = \frac{1}{4}$  is also substantially verified. By using different estimators of  $\eta$  we control the systematic error of our analysis, which turns out to be about 10%, and within about 10% our estimates of  $\eta$  are always consistent with the value  $\eta = \frac{1}{4}$ .

Substantial discrepancies from the Kosterlitz-Thouless theory are found in the estimates of  $\theta$  we obtained on all lattices considered and using also different estimators. Our strong coupling analysis based on Dlog-PA's leads, similarly to the K-T prediction, to a small absolute value of  $\theta$ , but it would favor the value  $\theta \simeq -0.04$ , against the K-T value  $\theta = \frac{1}{16}$ . Our strong coupling estimate seems to pass the universality check by changing lattice and estimator. On the other hand, we suggest some caution in considering our strong coupling estimate of  $\theta$ . Given the smallness of its value, we cannot exclude that the observed discrepancy is due to systematic errors caused by the fact that Dlog-PA's cannot reproduce the correction  $O(\tau^{1/2} \ln \tau)$  to the leading  $\tau^{-\theta}$  behavior in formula (25). Since this correction is expected to be present in all quantities we considered to estimate  $\theta$  (even when defined on different lattices), if its coefficients in the various cases are quantitatively similar the error might be about the same, and explain the apparent universality of our results. Moreover, the more general analysis based on IA's does not provide sufficiently stable results when applied to estimate  $\theta$ , likely because the available series are not sufficiently long to this purpose. We mention that in Ref. [17] an analysis based on Monte Carlo simulations led to the estimate  $\theta \simeq 0.02$ , which is not consistent with both the K-T prediction and our strong coupling estimate.

### III. LOW-MOMENTUM BEHAVIOR OF $G(x)$ IN THE CRITICAL REGION

In this section we study the low-momentum behavior of the two-point fundamental Green's function in the critical limit of the symmetric phase. To this purpose, we consider the dimensionless renormalization-group invariant function

$$L(p; \beta) \equiv \frac{\tilde{G}(0; \beta)}{\tilde{G}(p; \beta)}. \quad (26)$$

In the critical region of the symmetric phase  $L(p, \beta)$  is a function of the ratio  $y \equiv p^2/M_G^2$  only, where  $M_G \equiv 1/\xi_G$  and  $\xi_G \equiv m_2/4\chi$  is the second moment correlation length, already introduced in the previous section.  $L(y)$  can be expanded in powers of  $y$  around  $y = 0$ :

$$\begin{aligned} L(y) &= 1 + y + l(y) \\ l(y) &= \sum_{i=2}^{\infty} c_i y^i. \end{aligned} \quad (27)$$

$l(y)$  parameterizes the difference from a generalized Gaussian propagator. The coefficients  $c_i$  of the low-momentum expansion of  $l(y)$  can be related to appropriate dimensionless renormalization-group invariant ratios of moments  $m_{2j} = \sum_x (x^2)^j G(x)$ . Let us introduce the quantities

$$v_{2j} = \frac{1}{2^{2j}(j!)^2} M_G^{2j} \frac{m_{2j}}{m_0} \quad (28)$$

whose continuum limit is

$$v_{2j}^* = \frac{(-1)^j}{j!} \frac{d}{dy^j} L(y)^{-1} \Big|_{y=0}. \quad (29)$$

$v_{2j}^* = 1$  for a Gaussian critical propagator. One can easily write the coefficients  $c_i$  in terms of  $v_{2j}^*$ :

$$\begin{aligned} c_2 &= 1 - v_4^*, \\ c_3 &= 1 - 2v_4^* + v_6^* \\ c_4 &= 1 + v_4^*(v_4^* - 3) + 2v_6^* - v_8^*, \end{aligned} \quad (30)$$

etc. The strong-coupling expansion of  $G(x)$  allows to calculate strong-coupling series of  $v_{2j}$ . Estimates of the coefficients  $c_i$  can then be obtained, as we shall see, from the analysis of the combinations of  $v_{2j}$  corresponding to the r.h.s. of (30).

Another quantity which characterizes the low-momentum behavior of  $L(y)$  is the ratio  $s = M^2/M_G^2$  where  $M$  is the mass-gap of the theory, i.e., the mass determining the long distance exponential behavior of  $G(x)$ . The values  $s^*$  of  $s$  in the critical limit is related to the zero  $y_0$  of  $L(y)$  closest to the origin: indeed  $y_0 = -s^*$ .  $s^*$  is in general different from one; it is one in Gaussian-like models (i.e., when  $l(y) = 0$ ), such as the large- $N$  limit of  $O(N)$   $\sigma$  models, while no exact results are known at finite  $N$ .

In the absence of a strict rotation invariance, one may actually define different estimators of the mass-gap having the same continuum limit. On the square lattice one may consider  $\mu$  obtained by the long distance behavior of the side wall-wall correlation constructed with  $G(x)$ , or equivalently the solution of the equation  $\tilde{G}^{-1}(p_1 = i\mu, p_2 = 0) = 0$ . In view of a strong-coupling analysis, it is convenient to use another estimator of the mass-gap derived from  $\mu$ :

$$M_s^2 = 2(\cosh \mu - 1), \quad (31)$$

which has an ordinary strong-coupling expansion

$$M_s^2 = \frac{1}{\beta} \left( 1 + \sum_{i=1}^{\infty} a_i \beta^i \right) \quad (32)$$

( $\mu$  has a singular strong-coupling expansion, starting with  $-\ln \beta$ ). One can easily check that  $M_s/\mu \rightarrow 1$  in the critical limit. Similar quantities  $M_t^2$  and  $M_h^2$  can be defined respectively on the triangular and honeycomb lattices, as shown in Apps. B and C. One may then consider the dimensionless ratios  $M_s^2/M_G^2$ ,  $M_t^2/M_G^2$  and  $M_h^2/M_G^2$  respectively on the square, triangular and honeycomb lattices, and evaluate their fixed point limit  $s^*$ , which by universality must be the same for all of them. From the available strong-coupling series of  $M_s^2$  and  $M_G^2$  on the square lattice,  $M_t^2$  and  $M_G^2$  on the triangular lattice,  $M_h^2$  and  $M_G^2$  on the honeycomb lattice, which are reported, for  $N = 0, 1, 2$ , in Apps. A, B, C respectively, we computed the ratio  $M_s^2/M_G^2$  up to 16th order,  $M_t^2/M_G^2$  up to 11th order,  $M_h^2/M_G^2$  up to 25th order. For the Ising models, using the known exact results for  $M_s^2$ ,  $M_t^2$ , and  $M_h^2$  (see next section), we obtained longer series, i.e.  $M_s^2/M_G^2$  up to 20th order,  $M_t^2/M_G^2$  up to 14th order,  $M_h^2/M_G^2$  up to 29th order.

In order to determine  $s^*$ , and the coefficients  $c_i$  of the low-momentum expansion of  $L(y)$ , we analyzed the strong-coupling series of the ratios  $M_s^2/M_G^2$ ,  $M_t^2/M_G^2$  and  $M_h^2/M_G^2$ , and of the combinations of  $v_{2j}$  given in Eq. (30). Beside the ordinary series in  $\beta$ , we also considered and analyzed the corresponding series in the energy. The change of variable from  $\beta$  to the energy  $E$  is easily performed by inverting the strong-coupling series of the energy  $E = \beta + O(\beta^3)$  and substituting into the original series in powers of  $\beta$ . We constructed PA's and Dlog-PA's (and sometimes as further check also IA's) of both the series in  $\beta$  and in  $E$ . While PA's provide directly the quantity at hand, in a Dlog-PA analysis one gets corresponding approximants by reconstructing the original quantity from the PA of its logarithmic derivative. Estimates at criticality are then obtained by evaluating the approximants of the  $\beta$ -series at  $\beta_c$ , and those of the  $E$ -series at  $E_c$ , i.e., the value of the energy at  $\beta_c$ . In the cases in which  $E_c$  is not known from independent studies, its estimate may be derived from the first real positive singularity detected in the analysis of the strong-coupling series of  $\chi$ , or  $l_\chi$  for  $N = 2$ , expressed in powers of  $E$ .

In our analysis we considered quasi-diagonal  $[l/m]$  PA's and Dlog-PA's of the available series; more precisely, for a  $n$ th order series we considered those with

$$l, m \geq \frac{n}{2} - 2, \quad l + m \geq n - 2. \quad (33)$$

As a final estimate from each analysis we take the average of the results from the quasi-diagonal PA's and Dlog-PA's using all available terms of the series. The errors we display are the square root of the variance around the estimate of the results from all non-defective PA's indicated by Eq.(33).

By analyzing the above-mentioned series at  $N = 0, 1, 2$  we obtained estimates of  $s^*$ , and of some of the coefficients  $c_i$ . The results for  $N = 2$ , i.e., for the XY model, are reported in Table VII, those for  $N = 1, 0$  in Table VIII. Universality among the square, triangular and honeycomb lattices is in all cases well verified and gives further support to our final estimates.

For the XY model, the analysis of the  $E$ -series provides the most precise results on all lattices considered, leading to the estimates:

$$\begin{aligned} s^* &= 0.9985(5), \\ c_2 &= -1.5(5) \times 10^{-3}, \\ c_3 &= 2(2) \times 10^{-5}. \end{aligned} \quad (34)$$

The errors displayed are a rough estimate of the uncertainty.

For the Ising model, the two-point function in the scaling region is known analytically [28]. We obtained a benchmark for our strong-coupling computation by computing numerically the two-point function, following Ref. [28], and performing a numerical integration of the results:

$$\begin{aligned} s^* &\cong 0.99919633, \\ c_2 &\cong -0.7936796 \times 10^{-3}, \\ c_3 &\cong 1.095991 \times 10^{-5}, \\ c_4 &\cong -3.12747 \times 10^{-7}, \end{aligned} \quad (35)$$

The analysis of the available strong coupling series on the square, triangular and honeycomb lattices lead to the final estimates:

$$\begin{aligned} s^* &= 0.99908(3), \\ c_2 &= -0.94(4) \times 10^{-3}, \\ c_3 &= 1.1(3) \times 10^{-5}. \end{aligned} \quad (36)$$

The agreement with the exact results (35) is satisfactory. But the comparison shows also that the errors on the strong coupling estimates of  $s^*$  and  $c_2$ , essentially calculated using the variance of results from different PA's, are underestimated. We mention an earlier attempt to estimate  $s^*$  for the Ising model by using shorter strong-coupling series on the square and triangular lattices [29].

For the self-avoiding random walk model we find:

$$\begin{aligned} s^* &= 1.0000(2), \\ c_2 &= 0.13(6) \times 10^{-3}, \\ |c_3| &\lesssim 2 \times 10^{-5}. \end{aligned} \quad (37)$$

The analysis of the coefficients  $c_i$  with  $i > 3$  becomes less and less precise with increasing  $i$ , but it is consistent with very small values. For instance, we found in all cases  $|c_4| \lesssim |c_3|$ .

So, for all  $N$  considered, our strong-coupling analysis leads to the following pattern of the coefficients  $c_i$

$$c_i \ll c_2 \ll 1 \quad \text{for } i \geq 3. \quad (38)$$

This was also observed in models with  $N \geq 3$  by a study based on large- $N$  and strong-coupling calculations [6]. As a consequence of (38), the value of  $s^*$  should be essentially fixed by the term proportional to  $(p^2)^2$  in the inverse propagator, through the approximate relation

$$s^* - 1 \simeq c_2. \quad (39)$$

This equation is satisfied within the precision of our analysis for  $N = 0, 2$ , and well verified by the exact results of the Ising model, where  $s^* - 1 - c_2 \simeq 10^{-5}$ .

We can conclude that, like models with  $N \geq 3$ , in the critical region the two-point Green's function for  $N \leq 2$  is almost Gaussian in a large region around  $p^2 = 0$ , i.e.,  $|p^2/M_G^2| \lesssim 1$ , and the small corrections to Gaussian behavior are essentially determined by the  $(p^2)^2$  term in the expansion of the inverse propagator.

Differences from Gaussian behavior will become important at sufficiently large momenta, where  $G(p)$  should behave as

$$G(p) \sim \frac{1}{p^{2-\eta}} \quad (40)$$

where  $\eta \neq 0$ :  $\eta = \frac{5}{24}$  for  $N = 0$ , and  $\eta = \frac{1}{4}$  for  $N = 1, 2$ .

#### IV. LOW-MOMENTUM BEHAVIOR OF THE ISING MODEL

So far we considered only the critical limit of the two-point Green's function. It has however been known for a long time that the correlation functions of the two-dimensional Ising model can be computed exactly for arbitrary values of  $\beta$ . As a consequence we may in principle check directly our computations for every individual coordinate-space Green's function. In practice we may perform our checks by exploiting a peculiar feature of the square lattice solution: for sufficiently large values of  $\sqrt{x^2 + y^2}$  (in units of the lattice spacing) the asymptotic behavior is described by [30]

$$G(x, y) \simeq \left[ (1 - z^2)^2 - 4z^2 \right]^{1/4} (1 + z^2)^{1/2} (1 - z^2) \times \int \frac{d\phi_1}{2\pi} \frac{d\phi_2}{2\pi} \frac{e^{i\phi_1 x + i\phi_2 y}}{(1 + z^2)^2 - 2z(1 - z^2)(\cos \phi_1 + \cos \phi_2)}, \quad (41)$$

where we have introduced the auxiliary variable

$$z(\beta) = \tanh \beta. \quad (42)$$

We recognize that the above result (41) corresponds to the behavior of a nearest-neighbor quasi-Gaussian model whose momentum-space propagator has the form

$$\tilde{G}(p) = \frac{Z(\beta)}{\hat{p}^2 + M^2(\beta)} [1 + g(p, \beta)], \quad (43)$$

where  $g(p, \beta)$  vanishes at the pole  $\hat{p}^2 = -M^2(\beta)$ ,

$$Z(\beta) = \left[ (1 - z^2)^2 - 4z^2 \right]^{1/4} \frac{(1 + z^2)^{1/2}}{z}, \quad (44)$$

and

$$M^2(\beta) = \frac{(1 + z^2)^2}{z(1 - z^2)} - 4. \quad (45)$$

A straightforward but yet unobserved consequence of this observation is the algebraic relationship

$$2(\cosh \mu_s - 1) = 4(\cosh \frac{1}{2} \mu_d - 1) = M^2(\beta), \quad (46)$$

where  $\mu_s$  and  $\mu_d$  are the coefficients of the long-distance exponential decay (“true mass-gap”) on the side and along the principal diagonal of the square lattice. We verified that Eq. (46) is satisfied by our determinations of masses from wall-wall correlations and is consistent with the known relationship [29]

$$\mu_s = \ln \coth \beta - 2\beta. \quad (47)$$

We also checked that the residue at the pole  $\hat{p}^2 = -M^2$  satisfies Eq. (44).

Motivated by this piece of evidence we investigated the possibility that the asymptotic behavior of the two-point Green's function of the Ising model on regular two-dimensional lattices be always dictated by the structure of the propagator

$$\tilde{G}(p) = \frac{Z(\beta)}{\bar{p}^2 + M^2(\beta)} [1 + g(p, \beta)], \quad (48)$$

where  $\bar{p}^2$  is the massless (nearest-neighbor) Gaussian inverse propagator appropriate to the lattice at hand, and  $g(p, \beta)$  vanishes at the pole  $\bar{p}^2 = -M^2(\beta)$ . This conjecture can be checked by considering the large-distance behavior of the correlations for the triangular and honeycomb lattices, as a function of the direction, and comparing the different available mass definitions with each other and with exact results.

On the triangular lattice we can define a “true mass-gap”  $\mu_l$  from the asymptotic behavior of correlations taken along a straight line of links and a wall-wall inverse correlation length  $\mu_t$  evaluated in a direction orthogonal to the above defined line (see App. B). In a Gaussian model one would obtain

$$M_t^2 \equiv \frac{8}{3} \left( \cosh \frac{\sqrt{3}}{2} \mu_t - 1 \right) = \frac{8}{3} \left( \cosh \frac{1}{2} \mu_l - 1 \right) \left( \cosh \frac{1}{2} \mu_l + 2 \right). \quad (49)$$

Starting from the known solution [31]

$$\mu_l = 2 \ln \left( \sqrt{1 - z + z^2} - \sqrt{z} \right) - 2 \ln(1 - z) - \ln z, \quad (50)$$

we checked that the relationship (49) is satisfied, since our series for  $\mu_t$  reproduces the expansion of

$$M_t^2 = \frac{2}{3} \left[ \left( \frac{1+z^2}{1-z} \right)^2 \frac{1}{z} - 8 \right]. \quad (51)$$

Finally on the honeycomb lattice two mutually orthogonal inverse correlation lengths can be defined by the relationships

$$\begin{aligned} M_v^2 &= \frac{8}{9} \left( \cosh \frac{3}{2} \mu_v - 1 \right), \\ M_h^2 &= \frac{8}{3} \left( \cosh \frac{\sqrt{3}}{2} \mu_h - 1 \right), \end{aligned} \quad (52)$$

where  $\mu_v$  and  $\mu_h$  are defined from the large-distance exponential behavior respectively of wall-wall correlation functions  $G_v^{(w)}(x)$  and  $G_h^{(w)}(x)$  defined in App. C. The Gaussian relationship is

$$M_v^2 + 2 = \frac{1}{8} \left( M_h^2 + 4 \right)^2. \quad (53)$$

Moreover from duality with the weak coupling phase of the triangular lattice model we obtained

$$\mu_h = \frac{1}{\sqrt{3}} \left[ \ln \frac{\sqrt{2\cosh 2\beta - 1} - 1}{\sqrt{2\cosh 2\beta - 1} + 1} + 2\beta \right] \quad (54)$$

and we checked that the expansion of the  $M_h^2$  is consistent with

$$M_h^2 = \frac{4}{3} (2\cosh 2\beta - 1)^{1/2} \coth \beta - 4, \quad (55)$$

while Eq. (53) is satisfied to all known orders of the strong coupling expansion.

In conclusion we may say that the quasi-Gaussian structure of the propagator, described by Eq. (48), is confirmed for all regular lattices and is a remarkable piece of evidence in favor of adopting the quantities  $M^2$ ,  $M_t^2$  and  $M_h^2$  respectively as strong-coupling estimators of the mass-gap, sharing the property of a well-behaved  $\beta$ -dependence and of a faster approach to universality in models with quasi-Gaussian behavior. It is probably worth observing that, since  $g(0, \beta) \neq 0$ , Eq. (48) does not allow an immediate identification of the moments  $m_{2j}$ , and in particular  $M_G^2 \neq M^2$ , and  $Z(\beta)$  is not the standard zero-momentum wave function renormalization but corresponds to the on-shell definition.

## APPENDIX A: STRONG-COUPING SERIES ON THE SQUARE LATTICE

In order to enable the interested readers to perform their own analysis, we present most of the series used to derive the results presented in this paper for  $N = 0, 1, 2$ . This appendix is devoted to the square lattice, the following ones to the triangular and honeycomb lattices.

### 1. $N = 0$

For the self-avoiding random walk on the square lattice, longer series of  $M_G^2$  can be obtained from the strong-coupling series of  $\chi$  and  $m_2$  presented in Ref. [24]. We report our series of  $M_G^2$  for sake of completeness.

$$\begin{aligned} M_G^2 = & \beta^{-1} - 4 + 3\beta + 2\beta^3 + 4\beta^4 - 10\beta^5 + 48\beta^6 - 128\beta^7 + 368\beta^8 - 822\beta^9 + 2008\beta^{10} \\ & - 4320\beta^{11} + 10336\beta^{12} - 22800\beta^{13} + 56312\beta^{14} - 129922\beta^{15} + 327080\beta^{16} - 768414\beta^{17} \\ & + 1938440\beta^{18} - 4604254\beta^{19} + O(\beta^{20}), \end{aligned} \quad (A1a)$$

$$\begin{aligned} M_s^2 = & \beta^{-1} - 4 + 3\beta + 2\beta^3 + 4\beta^4 - 8\beta^5 + 30\beta^6 - 52\beta^7 + 140\beta^8 - 234\beta^9 + 596\beta^{10} \\ & - 1010\beta^{11} + 2638\beta^{12} - 4644\beta^{13} + 12634\beta^{14} - 23208\beta^{15} + O(\beta^{16}), \end{aligned} \quad (A1b)$$

$$\begin{aligned} v_4 = & \frac{1}{16}\beta^{-1} + \frac{3}{4} + \frac{3}{16}\beta + \frac{1}{8}\beta^3 + \frac{3}{8}\beta^5 - \beta^6 + \frac{15}{2}\beta^7 - 19\beta^8 + \frac{409}{8}\beta^9 - 103\beta^{10} + \frac{511}{2}\beta^{11} \\ & - 539\beta^{12} + 1468\beta^{13} - 3649\beta^{14} + \frac{83211}{8}\beta^{15} - 25668\beta^{16} + \frac{534225}{8}\beta^{17} - 154972\beta^{18} \\ & + \frac{3095629}{8}\beta^{19} + O(\beta^{20}). \end{aligned} \quad (A1c)$$

### 2. $N = 1$

For the Ising model we give strong coupling series which cannot be reproduced using known exact results, which are reported in Sec. IV.

$$\begin{aligned}
M_G^2 = & \beta^{-1} - 4 + \frac{10}{3}\beta + \frac{134}{45}\beta^3 + \frac{76}{189}\beta^5 + \frac{19394}{4725}\beta^7 - 32\beta^8 + \frac{2070328}{18711}\beta^9 - \frac{704}{3}\beta^{10} \\
& + \frac{233105490328}{638512875}\beta^{11} - \frac{20656}{45}\beta^{12} + \frac{440148292}{729729}\beta^{13} - \frac{256064}{189}\beta^{14} + \frac{670306901872438}{162820783125}\beta^{15} - \frac{52233344}{4725}\beta^{16} \\
& + \frac{192016952587260544}{7795859096025}\beta^{17} - \frac{4476104704}{93555}\beta^{18} + \frac{133522860364557505628}{1531329465290625}\beta^{19} + O(\beta^{20}),
\end{aligned} \tag{A2a}$$

$$\begin{aligned}
v_4 = & \frac{1}{16}\beta^{-1} + \frac{3}{4} + \frac{5}{24}\beta + \frac{67}{360}\beta^3 + \frac{19}{756}\beta^5 + \frac{9697}{37800}\beta^7 + 2\beta^8 - \frac{339961}{37422}\beta^9 + \frac{44}{3}\beta^{10} + \frac{8705774291}{1277025750}\beta^{11} \\
& - \frac{4514}{45}\beta^{12} + \frac{3986722469}{14594580}\beta^{13} - \frac{68668}{189}\beta^{14} - \frac{115832206185781}{1302566265000}\beta^{15} + \frac{6752894}{4725}\beta^{16} \\
& - \frac{21607992820912952}{7795859096025}\beta^{17} + \frac{34100716}{93555}\beta^{18} + \frac{71772260149691061407}{6125317861162500}\beta^{19} + O(\beta^{20}).
\end{aligned} \tag{A2b}$$

### 3. $N = 2$

$$\begin{aligned}
E = & \beta + \frac{3}{2}\beta^3 + \frac{1}{3}\beta^5 - \frac{31}{48}\beta^7 - \frac{731}{120}\beta^9 - \frac{29239}{1440}\beta^{11} - \frac{265427}{5040}\beta^{13} - \frac{75180487}{645120}\beta^{15} - \frac{6506950039}{26127360}\beta^{17} \\
& - \frac{1102473407093}{2612736000}\beta^{19} - \frac{6986191770643}{14370048000}\beta^{21} + O(\beta^{23}),
\end{aligned} \tag{A3a}$$

$$\begin{aligned}
\chi = & 1 + 4\beta + 12\beta^2 + 34\beta^3 + 88\beta^4 + \frac{658}{3}\beta^5 + 529\beta^6 + \frac{14933}{12}\beta^7 + \frac{5737}{2}\beta^8 + \frac{389393}{60}\beta^9 \\
& + \frac{2608499}{180}\beta^{10} + \frac{3834323}{120}\beta^{11} + \frac{1254799}{18}\beta^{12} + \frac{84375807}{560}\beta^{13} + \frac{6511729891}{20160}\beta^{14} + \frac{66498259799}{96768}\beta^{15} \\
& + \frac{1054178743699}{725760}\beta^{16} + \frac{39863505993331}{13063680}\beta^{17} + \frac{19830277603399}{3110400}\beta^{18} + \frac{8656980509809027}{653184000}\beta^{19} \\
& + \frac{2985467351081077}{108864000}\beta^{20} + \frac{811927408684296587}{14370048000}\beta^{21} + O(\beta^{22}),
\end{aligned} \tag{A3b}$$

$$\begin{aligned}
M_G^2 = & \beta^{-1} - 4 + \frac{7}{2}\beta + \frac{41}{12}\beta^3 - \beta^4 + \frac{15}{16}\beta^5 - \frac{25}{3}\beta^6 + \frac{9491}{720}\beta^7 - \frac{431}{9}\beta^8 + \frac{206411}{2880}\beta^9 - \frac{17803}{360}\beta^{10} \\
& - \frac{41122019}{241920}\beta^{11} + \frac{876403}{1728}\beta^{12} - \frac{1413373319}{1935360}\beta^{13} - \frac{15006841}{181440}\beta^{14} + \frac{337093786457}{130636800}\beta^{15} - \frac{4777620367}{1036800}\beta^{16} \\
& + \frac{17847363647}{1741824000}\beta^{17} + \frac{68513340691}{3732480}\beta^{18} - \frac{16133717627082721}{344881152000}\beta^{19} + O(\beta^{20}),
\end{aligned} \tag{A3c}$$

$$\begin{aligned}
M_s^2 = & \beta^{-1} - 4 + \frac{7}{2}\beta + \frac{41}{12}\beta^3 - \beta^4 + \frac{7}{16}\beta^5 - \frac{29}{6}\beta^6 + \frac{281}{720}\beta^7 - \frac{193}{18}\beta^8 - \frac{149}{2880}\beta^9 - \frac{5141}{720}\beta^{10} \\
& - \frac{6120227}{241920}\beta^{11} + \frac{24907}{540}\beta^{12} - \frac{788579333}{5806080}\beta^{13} + \frac{95728039}{362880}\beta^{14} - \frac{63069969313}{130636800}\beta^{15} + O(\beta^{16}),
\end{aligned} \tag{A3d}$$

$$\begin{aligned}
v_4 = & \frac{1}{16}\beta^{-1} + \frac{3}{4} + \frac{7}{32}\beta + \frac{41}{192}\beta^3 - \frac{49}{256}\beta^5 + \frac{1}{4}\beta^6 - \frac{8749}{11520}\beta^7 + \frac{67}{48}\beta^8 - \frac{122549}{46080}\beta^9 - \frac{2153}{144}\beta^{10} \\
& + \frac{249335197}{3870720}\beta^{11} - \frac{40951}{320}\beta^{12} + \frac{1389732217}{30965760}\beta^{13} + \frac{55582271}{103680}\beta^{14} - \frac{3706449404743}{2090188800}\beta^{15} + \frac{6252985429}{2903040}\beta^{16} \\
& + \frac{75252500337407}{27869184000}\beta^{17} - \frac{202521546511}{12441600}\beta^{18} + \frac{163636654204247999}{5518098432000}\beta^{19} + O(\beta^{20}).
\end{aligned} \tag{A3e}$$

## APPENDIX B: STRONG-COUPING SERIES ON THE TRIANGULAR LATTICE

The sites  $\vec{x}$  of a finite periodic triangular lattice can be represented in Cartesian coordinates by

$$\begin{aligned}
\vec{x}(l_1, l_2) &= l_1\vec{\eta}_1 + l_2\vec{\eta}_2, \\
l_1 &= 1, \dots, L_1, \quad l_2 = 1, \dots, L_2, \\
\vec{\eta}_1 &= (1, 0), \quad \vec{\eta}_2 = \left(\frac{1}{2}, \frac{\sqrt{3}}{2}\right).
\end{aligned} \tag{B1}$$

In order to define a mass-gap estimator, one may consider the following wall-wall correlation function

$$G_t^{(w)} \left( \frac{\sqrt{3}}{2} l_2 \right) = \sum_{l_1} G(l_1 \vec{\eta}_1 + l_2 \vec{\eta}_2). \quad (B2)$$

An estimator  $\mu_t$  of the mass-gap can be extracted from the long distance behavior of  $G_t^{(w)}(x)$ , indeed for  $x \gg 1$

$$G_t^{(w)}(x) \propto e^{-\mu_t x}. \quad (B3)$$

In view of a strong-coupling analysis, it is convenient to use another estimator of the mass-gap derived from  $\mu_t$ :

$$M_t^2 \equiv \frac{8}{3} \left( \cosh \frac{\sqrt{3}}{2} \mu_t - 1 \right). \quad (B4)$$

More details can be found in Ref. [6].

In the following we show, for  $N = 0, 1, 2$ , some of the strong-coupling series used in the analysis of the  $O(N)$   $\sigma$  models on the triangular lattice presented in this paper.

## 1. $N = 0$

For the self-avoiding random walk on the triangular lattice, longer series of  $M_G^2$  can be obtained from the strong-coupling series of  $\chi$  and  $m_2$  presented in Ref. [25].

$$\begin{aligned} M_G^2 = & \frac{2}{3} \beta^{-1} - 4 + \frac{10}{3} \beta + 4\beta^2 + \frac{16}{3} \beta^3 + \frac{40}{3} \beta^4 + \frac{88}{3} \beta^5 + \frac{88}{3} \beta^6 + 228 \beta^7 + \frac{1808}{3} \beta^8 + \frac{4352}{3} \beta^9 \\ & + \frac{18356}{3} \beta^{10} + \frac{52792}{3} \beta^{11} + 60540 \beta^{12} + \frac{631184}{3} \beta^{13} + O(\beta^{14}), \end{aligned} \quad (B5a)$$

$$\begin{aligned} M_t^2 = & \frac{2}{3} \beta^{-1} - 4 + \frac{10}{3} \beta + 4\beta^2 + \frac{17}{3} \beta^3 + \frac{35}{3} \beta^4 + \frac{47}{2} \beta^5 + \frac{205}{3} \beta^6 + 188 \beta^7 + \frac{2213}{4} \beta^8 + \frac{41909}{24} \beta^9 \\ & + \frac{33181}{6} \beta^{10} + O(\beta^{11}), \end{aligned} \quad (B5b)$$

$$\begin{aligned} v_4 = & \frac{1}{24} \beta^{-1} + \frac{3}{4} + \frac{5}{24} \beta + \frac{1}{4} \beta^2 + \frac{1}{3} \beta^3 + \frac{1}{3} \beta^4 + \frac{4}{3} \beta^5 + \frac{59}{6} \beta^6 + \frac{55}{4} \beta^7 + \frac{98}{3} \beta^8 + \frac{1135}{6} \beta^9 \\ & + \frac{4529}{12} \beta^{10} + \frac{4783}{3} \beta^{11} + \frac{21295}{4} \beta^{12} + \frac{100165}{6} \beta^{13} + O(\beta^{14}). \end{aligned} \quad (B5c)$$

## 2. $N = 1$

For the Ising model we give strong coupling series which cannot be reproduced using known exact results.

$$\begin{aligned} M_G^2 = & \frac{2}{3} \beta^{-1} - 4 + \frac{32}{9} \beta + \frac{16}{3} \beta^2 + \frac{928}{135} \beta^3 + \frac{64}{9} \beta^4 + \frac{23944}{2835} \beta^5 - \frac{1648}{135} \beta^6 + \frac{5008}{14175} \beta^7 + \frac{106864}{945} \beta^8 \\ & + \frac{6459424}{280665} \beta^9 - \frac{18680128}{42525} \beta^{10} - \frac{200433692584}{1915538625} \beta^{11} + \frac{2151999728}{1403325} \beta^{12} + \frac{35136345008}{54729675} \beta^{13} + O(\beta^{14}), \end{aligned} \quad (B6a)$$

$$\begin{aligned} v_4 = & \frac{1}{24} \beta^{-1} + \frac{3}{4} + \frac{2}{9} \beta + \frac{1}{3} \beta^2 + \frac{58}{135} \beta^3 + \frac{4}{9} \beta^4 + \frac{2993}{5670} \beta^5 + \frac{437}{135} \beta^6 + \frac{313}{14175} \beta^7 - \frac{19781}{945} \beta^8 \\ & + \frac{403714}{280665} \beta^9 + \frac{3986522}{42525} \beta^{10} - \frac{354526855073}{3831077250} \beta^{11} - \frac{960767707}{1403325} \beta^{12} - \frac{18090444637}{54729675} \beta^{13} + O(\beta^{14}). \end{aligned} \quad (B6b)$$

### 3. $N = 2$

$$E = \beta + 2\beta^2 + \frac{7}{2}\beta^3 + 5\beta^4 + \frac{35}{6}\beta^5 + \frac{14}{3}\beta^6 - \frac{81}{16}\beta^7 - \frac{3769}{72}\beta^8 - \frac{165161}{720}\beta^9 - \frac{7821}{10}\beta^{10} - \frac{20160371}{8640}\beta^{11} - \frac{27984359}{4320}\beta^{12} - \frac{87289819}{5040}\beta^{13} - \frac{10256893919}{226800}\beta^{14} - \frac{3357272555039}{29030400}\beta^{15} + O(\beta^{16}), \quad (B7a)$$

$$\begin{aligned} \chi = 1 + 6\beta + 30\beta^2 + 135\beta^3 + 570\beta^4 + 2306\beta^5 + \frac{18083}{2}\beta^6 + \frac{276657}{8}\beta^7 + \frac{777805}{6}\beta^8 \\ + \frac{14339641}{30}\beta^9 + \frac{208590287}{120}\beta^{10} + \frac{8995595389}{1440}\beta^{11} + \frac{3199713875}{144}\beta^{12} + \frac{65793037351}{840}\beta^{13} \\ + \frac{165647319078571}{604800}\beta^{14} + \frac{4600845479023849}{4838400}\beta^{15} + O(\beta^{16}), \end{aligned} \quad (B7b)$$

$$\begin{aligned} M_G^2 = \frac{2}{3}\beta^{-1} - 4 + \frac{11}{3}\beta + 6\beta^2 + \frac{143}{18}\beta^3 + \frac{46}{9}\beta^4 - \frac{391}{72}\beta^5 - \frac{5219}{108}\beta^6 - \frac{5296}{45}\beta^7 - \frac{33287}{180}\beta^8 \\ - \frac{679729}{1296}\beta^9 - \frac{2052143}{1080}\beta^{10} - \frac{1436935039}{362880}\beta^{11} - \frac{4952351659}{1360800}\beta^{12} - \frac{87992319949}{43545600}\beta^{13} + O(\beta^{14}) \end{aligned} \quad (B7c)$$

$$\begin{aligned} M_t^2 = \frac{2}{3}\beta^{-1} - 4 + \frac{11}{3}\beta + 6\beta^2 + \frac{283}{36}\beta^3 + \frac{49}{9}\beta^4 - \frac{53}{8}\beta^5 - \frac{8425}{216}\beta^6 - \frac{990757}{8640}\beta^7 - \frac{45549}{160}\beta^8 \\ - \frac{16833083}{25920}\beta^9 - \frac{35865709}{25920}\beta^{10} + O(\beta^{11}), \end{aligned} \quad (B7d)$$

$$\begin{aligned} v_4 = \frac{1}{24}\beta^{-1} + \frac{3}{4} + \frac{11}{48}\beta + \frac{3}{8}\beta^2 + \frac{143}{288}\beta^3 + \frac{4}{9}\beta^4 - \frac{103}{1152}\beta^5 - \frac{827}{1728}\beta^6 - \frac{6271}{720}\beta^7 - \frac{39709}{960}\beta^8 \\ - \frac{1243813}{20736}\beta^9 + \frac{85031}{3456}\beta^{10} - \frac{741356239}{5806080}\beta^{11} - \frac{7581779911}{5443200}\beta^{12} - \frac{1477616543629}{696729600}\beta^{13} + O(\beta^{14}). \end{aligned} \quad (B7e)$$

## APPENDIX C: STRONG-COUPING SERIES ON THE HONEYCOMB LATTICE

The sites  $\vec{x}$  of a finite periodic honeycomb lattice can be represented in Cartesian coordinates by

$$\begin{aligned} \vec{x} &= \vec{x}' + p\vec{\eta}_p \\ \vec{x}' &= l_1\vec{\eta}_1 + l_2\vec{\eta}_2, \\ l_1 &= 1, \dots, L_1, \quad l_2 = 1, \dots, L_2, \quad p = 0, 1, \\ \vec{\eta}_1 &= \left(\frac{3}{2}, \frac{\sqrt{3}}{2}\right), \quad \vec{\eta}_2 = (0, \sqrt{3}), \quad \vec{\eta}_p = (1, 0). \end{aligned} \quad (C1)$$

In order to define a mass-gap estimator, one may consider the following wall-wall correlation functions

$$G_v^{(w)}\left(\frac{3}{2}l_1\right) = \sum_{l_2} G(l_1\vec{\eta}_1 + l_2\vec{\eta}_2), \quad (C2)$$

with the sum running over sites of positive parity forming a vertical line;

$$G_h^{(w)}\left(\frac{1}{2}\sqrt{3}l\right) = \sum_{l_2, p} G((l - 2l_2)\vec{\eta}_1 + l_2\vec{\eta}_2 + p\vec{\eta}_p), \quad (C3)$$

where the sum is performed over all sites having the same coordinate  $x_2$ .

Estimators  $\mu_v$  and  $\mu_h$  of the mass-gap can be extracted from the long distance behavior respectively of  $G_v^{(w)}(x)$  and  $G_h^{(w)}(x)$ , indeed for  $x \gg 1$

$$\begin{aligned} G_h^{(w)}(x) &\propto e^{-\mu_v x}, \\ G_h^{(w)}(x) &\propto e^{-\mu_h x}. \end{aligned} \quad (C4)$$

In view of a strong-coupling analysis, it is convenient to use the following estimators of the mass-gap derived from  $\mu_v$  and  $\mu_h$ :

$$\begin{aligned} M_v^2 &\equiv \frac{8}{9} \left( \cosh \frac{3}{2} \mu_h - 1 \right), \\ M_h^2 &\equiv \frac{8}{3} \left( \cosh \frac{\sqrt{3}}{2} \mu_h - 1 \right). \end{aligned} \quad (C5)$$

More details can be found in Ref. [6].

In the following we show, for  $N = 0, 1, 2$ , some of the strong-coupling series used in the analysis of  $O(N)$   $\sigma$  models on the honeycomb lattice presented in this paper.

## 1. $N = 0$

For the self-avoiding random walk on the honeycomb lattice, longer series of  $M_G^2$  can be obtained from the strong-coupling series of  $\chi$  and  $m_2$  presented in Ref. [24].

$$\begin{aligned} M_G^2 = & \frac{4}{3} \beta^{-1} - 4 + \frac{8}{3} \beta + 8 \beta^6 - \frac{56}{3} \beta^7 + 24 \beta^8 - 32 \beta^9 + 96 \beta^{10} - \frac{656}{3} \beta^{11} + 320 \beta^{12} - 296 \beta^{13} \\ & + 416 \beta^{14} - 1192 \beta^{15} + 2848 \beta^{16} - \frac{13304}{3} \beta^{17} + 5768 \beta^{18} - \frac{27664}{3} \beta^{19} + 20024 \beta^{20} - 38520 \beta^{21} \\ & + 63368 \beta^{22} - 100104 \beta^{23} + 183352 \beta^{24} - \frac{1039744}{3} \beta^{25} + 621096 \beta^{26} - \frac{3093176}{3} \beta^{27} \\ & + 1791168 \beta^{28} + O(\beta^{29}), \end{aligned} \quad (C6a)$$

$$\begin{aligned} M_h^2 = & \frac{4}{3} \beta^{-1} - 4 + \frac{8}{3} \beta + \frac{4}{3} \beta^5 + \frac{8}{3} \beta^9 + \frac{8}{3} \beta^{10} - 4 \beta^{11} + 8 \beta^{12} + \frac{16}{3} \beta^{13} + 8 \beta^{14} + \frac{8}{3} \beta^{15} + 16 \beta^{16} \\ & + \frac{148}{3} \beta^{17} + 36 \beta^{18} + \frac{176}{3} \beta^{19} + \frac{100}{3} \beta^{20} + \frac{1532}{3} \beta^{21} - 248 \beta^{22} + \frac{4348}{3} \beta^{23} - \frac{3184}{3} \beta^{24} + O(\beta^{25}), \\ v_4 = & \frac{1}{12} \beta^{-1} + \frac{3}{4} + \frac{1}{6} \beta - \frac{1}{2} \beta^6 + \frac{11}{6} \beta^7 - \frac{3}{2} \beta^8 + \beta^9 - 6 \beta^{10} + \frac{70}{3} \beta^{11} - 35 \beta^{12} + \frac{11}{2} \beta^{13} + 49 \beta^{14} \\ & + \frac{75}{2} \beta^{15} - 397 \beta^{16} + \frac{4631}{6} \beta^{17} - \frac{1051}{2} \beta^{18} - \frac{349}{3} \beta^{19} - \frac{1087}{2} \beta^{20} + \frac{8001}{2} \beta^{21} - \frac{15883}{2} \beta^{22} + \frac{17989}{2} \beta^{23} \\ & - \frac{19691}{2} \beta^{24} + \frac{72668}{3} \beta^{25} - \frac{112563}{2} \beta^{26} + \frac{536981}{6} \beta^{27} - 110355 \beta^{28} + O(\beta^{29}). \end{aligned} \quad (C6b)$$

## 2. $N = 1$

$$\begin{aligned} M_G^2 = & \frac{4}{3} \beta^{-1} - 4 + \frac{28}{9} \beta - \frac{124}{135} \beta^3 + \frac{8576}{2835} \beta^5 - \frac{14692}{2025} \beta^7 + \frac{5338616}{280665} \beta^9 - \frac{90947891648}{1915538625} \beta^{11} - 32 \beta^{12} \\ & + \frac{1583805616}{7818525} \beta^{13} + 96 \beta^{14} - \frac{406965884456828}{488462349375} \beta^{15} - \frac{608}{15} \beta^{16} + \frac{360870502928894432}{116937886440375} \beta^{17} - \frac{1219136}{945} \beta^{18} \\ & - \frac{6493740451647884584}{656284056553125} \beta^{19} + \frac{624064}{75} \beta^{20} + \frac{1179228814388026215376}{40343570821929375} \beta^{21} - \frac{5843265248}{155925} \beta^{22} \\ & - \frac{48910471162936574893856768}{605758715891269565625} \beta^{23} + \frac{405278723648}{2837835} \beta^{24} + \frac{1024764052182397586576416}{4754777989727390625} \beta^{25} \\ & - \frac{1697456183968}{3378375} \beta^{26} - \frac{950155935558179228231150591072}{1693960980510228821015625} \beta^{27} + \frac{54851554589151328}{32564156625} \beta^{28} + O(\beta^{29}), \end{aligned} \quad (C7a)$$

$$\begin{aligned} v_4 = & \frac{1}{12} \beta^{-1} + \frac{3}{4} + \frac{7}{36} \beta - \frac{31}{540} \beta^3 + \frac{536}{2835} \beta^5 - \frac{3673}{8100} \beta^7 + \frac{667327}{561330} \beta^9 - \frac{5684243228}{1915538625} \beta^{11} + 2 \beta^{12} \\ & + \frac{516551}{7818525} \beta^{13} - 6 \beta^{14} + \frac{93643468635793}{1953849397500} \beta^{15} - \frac{1042}{15} \beta^{16} - \frac{27120807726815398}{116937886440375} \beta^{17} + \frac{643196}{945} \beta^{18} \\ & + \frac{86312750362752061}{187509730443750} \beta^{19} - \frac{258424}{75} \beta^{20} + \frac{33629885325845121661}{40343570821929375} \beta^{21} + \frac{1973399678}{155925} \beta^{22} \\ & - \frac{6840786318771414403278548}{605758715891269565625} \beta^{23} - \frac{106606055168}{2837835} \beta^{24} + \frac{282271419983204843625526}{4754777989727390625} \beta^{25} + \frac{44788447114}{482625} \beta^{26} \\ & - \frac{402797762032926523234583974442}{1693960980510228821015625} \beta^{27} - \frac{599229992104838}{32564156625} \beta^{28} + O(\beta^{29}) \end{aligned} \quad (C7b)$$

### 3. $N = 2$

$$\begin{aligned}
E = & \beta - \frac{1}{2}\beta^3 + \frac{7}{3}\beta^5 - \frac{395}{48}\beta^7 + \frac{1173}{40}\beta^9 - \frac{473243}{4320}\beta^{11} + \frac{6293627}{15120}\beta^{13} - \frac{346093553}{215040}\beta^{15} \\
& + \frac{23497364693}{3732480}\beta^{17} - \frac{64962730739719}{2612736000}\beta^{19} + \frac{474090720713083}{4790016000}\beta^{21} - \frac{1641257090013388013}{4138573824000}\beta^{23} \\
& + \frac{42984420336380838389}{26900729856000}\beta^{25} - \frac{11369733294965786406529}{1757514350592000}\beta^{27} + \frac{1733398746685522588378351}{65906788147200000}\beta^{29} + O(\beta^{30}),
\end{aligned} \tag{C8a}$$

$$\begin{aligned}
\chi = & 1 + 3\beta + 6\beta^2 + \frac{21}{2}\beta^3 + 18\beta^4 + 31\beta^5 + \frac{95}{2}\beta^6 + \frac{1045}{16}\beta^7 + \frac{403}{4}\beta^8 + \frac{6919}{40}\beta^9 + \frac{14149}{60}\beta^{10} \\
& + \frac{68273}{288}\beta^{11} + \frac{138307}{360}\beta^{12} + \frac{9157051}{10080}\beta^{13} + \frac{42124273}{40320}\beta^{14} - \frac{13183321}{645120}\beta^{15} + \frac{130286011}{161280}\beta^{16} \\
& + \frac{58701184637}{8709120}\beta^{17} + \frac{246444397309}{43545600}\beta^{18} - \frac{12790078293739}{870912000}\beta^{19} - \frac{79551567889}{13608000}\beta^{20} + \frac{154021837152677}{1916006400}\beta^{21} \\
& + \frac{1452164594591761}{28740096000}\beta^{22} - \frac{393634368786168197}{1379524608000}\beta^{23} - \frac{4660955848386121}{31352832000}\beta^{24} + \frac{10915691174925870017}{8966909952000}\beta^{25} \\
& + \frac{41989311871750076949}{62768369664000}\beta^{26} - \frac{8481318776641386327367}{1757514350592000}\beta^{27} - \frac{828979117543657737823}{329533940736000}\beta^{28} \\
& + \frac{5226218120804763962092657}{263627152588800000}\beta^{29} + \frac{21701722199756349611186159}{2109017220710400000}\beta^{30} + O(\beta^{31}),
\end{aligned} \tag{C8b}$$

$$\begin{aligned}
M_G^2 = & \frac{4}{3}\beta^{-1} - 4 + \frac{10}{3}\beta - \frac{13}{9}\beta^3 + \frac{59}{12}\beta^5 - 2\beta^6 - \frac{3347}{270}\beta^7 + \frac{35}{6}\beta^8 + \frac{238009}{6480}\beta^9 - \frac{493}{18}\beta^{10} \\
& - \frac{19392227}{181440}\beta^{11} + \frac{4388}{45}\beta^{12} + \frac{1467214247}{4354560}\beta^{13} - \frac{3846767}{12960}\beta^{14} - \frac{245879581721}{195955200}\beta^{15} + \frac{362651221}{362880}\beta^{16} \\
& + \frac{6669774367471}{1306368000}\beta^{17} - \frac{45385487873}{10886400}\beta^{18} - \frac{5401824824719549}{258660864000}\beta^{19} + \frac{68257961593}{3483648}\beta^{20} \\
& + \frac{258003704533726433}{3103930368000}\beta^{21} - \frac{362403210060397}{3919104000}\beta^{22} - \frac{5054778739819764833}{15692092416000}\beta^{23} + \frac{72793501494263779}{172440576000}\beta^{24} \\
& + \frac{290687412809274634879279}{237264437329920000}\beta^{25} - \frac{202156253372553206149}{108637562880000}\beta^{26} - \frac{43738864245549216552954097}{9490577493196800000}\beta^{27} \\
& + \frac{45054828678355702664561}{5649153269760000}\beta^{28} + O(\beta^{29}),
\end{aligned} \tag{C8c}$$

$$\begin{aligned}
M_h^2 = & \frac{4}{3}\beta^{-1} - 4 + \frac{10}{3}\beta - \frac{13}{9}\beta^3 + \frac{55}{12}\beta^5 - \frac{1}{3}\beta^6 - \frac{7429}{540}\beta^7 - \frac{2}{9}\beta^8 + \frac{282139}{6480}\beta^9 - \frac{43}{216}\beta^{10} \\
& - \frac{26145491}{181440}\beta^{11} + \frac{613}{540}\beta^{12} + \frac{2158358071}{4354560}\beta^{13} - \frac{224587}{77760}\beta^{14} - \frac{344839817111}{195955200}\beta^{15} + \frac{1698299}{272160}\beta^{16} \\
& + \frac{8350838655511}{1306368000}\beta^{17} + \frac{63590671}{130636800}\beta^{18} - \frac{3061458683224637}{129330432000}\beta^{19} - \frac{1894590323}{52254720}\beta^{20} \\
& + \frac{39427276163585267}{443418624000}\beta^{21} + \frac{5154851721889}{23514624000}\beta^{22} - \frac{5303030533425785401}{15692092416000}\beta^{23} - \frac{174214610003233}{147806208000}\beta^{24} \\
& + O(\beta^{25}),
\end{aligned} \tag{C8d}$$

$$\begin{aligned}
v_4 = & \frac{1}{12}\beta^{-1} + \frac{3}{4} + \frac{5}{24}\beta - \frac{13}{144}\beta^3 + \frac{59}{192}\beta^5 + \frac{1}{8}\beta^6 - \frac{5507}{4320}\beta^7 - \frac{71}{96}\beta^8 + \frac{495049}{103680}\beta^9 + \frac{961}{288}\beta^{10} \\
& - \frac{47837987}{2903040}\beta^{11} - \frac{43397}{2880}\beta^{12} + \frac{4159541927}{69672960}\beta^{13} + \frac{11139143}{207360}\beta^{14} - \frac{643769125241}{3135283200}\beta^{15} - \frac{1093077841}{5806080}\beta^{16} \\
& + \frac{13258559750671}{20901888000}\beta^{17} + \frac{148926884453}{174182400}\beta^{18} - \frac{1148899892904427}{591224832000}\beta^{19} - \frac{6289014713053}{1393459200}\beta^{20} \\
& + \frac{353359211049440273}{49662885888000}\beta^{21} + \frac{202048769925301}{8957952000}\beta^{22} - \frac{2704447377391331531}{83691159552000}\beta^{23} - \frac{278880464307951691}{2759049216000}\beta^{24} \\
& + \frac{54781761414365119518029}{345111908843520000}\beta^{25} + \frac{715504863884795060149}{1738201006080000}\beta^{26} - \frac{10548822433407426077233907}{13804476353740800000}\beta^{27} \\
& - \frac{140706622546312581163859}{90386452316160000}\beta^{28} + O(\beta^{29}).
\end{aligned} \tag{C8e}$$

## REFERENCES

- [1] M. Campostrini, A. Pelissetto, P. Rossi and E. Vicari, “Strong coupling expansion of lattice  $O(N)$  sigma models” IFUP-TH 51/95, hep-lat/9509025, proceedings of the conference “Lattice 95”, Melbourne 1995, Nucl. Phys. **B** (Proc. Suppl.) in press; M. Campostrini, A. Cucchieri, T. Mendes, A. Pelissetto, P. Rossi, A. D. Sokal, and E. Vicari, “Application of the  $O(N)$  hyperspherical harmonics to the study of the continuum limits of one-dimensional sigma models and to the generation of high temperature expansions in higher dimensions”, NYU-TH-95-09-06, hep-lat/9509034, *ibid*.
- [2] M. Lüscher and P. Weisz, Nucl. Phys. **B300**, 325 (1988).
- [3] P. Butera, M. Comi, and G. Marchesini, Phys. Rev. **B 41**, 11494 (1990).
- [4] T. Reisz, Nucl. Phys. **B450**, 569 (1995).
- [5] P. Butera and M. Comi, “New extended high-temperature series for the  $N$ -vector spin models on three-dimensional bipartite lattices”, IFUM-TH 498, hep-lat/9505027 (1995).
- [6] M. Campostrini, A. Pelissetto, P. Rossi and E. Vicari, “A strong-coupling analysis of  $O(N)$   $\sigma$  models with  $N \geq 3$  on the square, triangular and honeycomb lattices”, IFUP-TH 5/96, hep-lat/9602011.
- [7] R. Balian and G. Toulouse, Phys. Rev. Lett. **30** 544 (1973).
- [8] J. Cardy and H. Hamber, Phys. Rev. Lett. **45** 499 (1980).
- [9] B. Nienhuis, Phys. Rev. Lett. **49** 1062 (1982); J. Stat. Phys. **34**, 731 (1984).
- [10] V. S. Dotsenko and V. A. Fateev, Nucl. Phys. **B240**, 312 (1984).
- [11] J. M. Kosterlitz and D. J. Thouless, J. Phys. **C 6**, 1181 (1973); J. M. Kosterlitz, **C 7**, 1046 (1974).
- [12] C. Itzykson and J. M. Drouffe, “Statistical field theory”, Cambridge University Press (Cambridge 1989).
- [13] M. Hasenbush, M. Marcu, and K. Pinn, Physica **A 208**, 124 (1994).
- [14] R. Gupta and C. F. Baillie, Phys. Rev. **D 45**, 2883 (1992).
- [15] J. Kim, “Crossover in the critical behavior of the two dimensional classical XY model”, hep-lat/9502002, (1995).
- [16] L. Biferale and R. Petronzio, Nucl. Phys. **B328**, 677 (1989).
- [17] R. Kenna and A. C. Irving, Phys. Lett. **351B**, 273 (1995); “The Kosterlitz-Thouless universality class”, hep-lat/9601029 (1996).
- [18] P. Butera and M. Comi, Phys. Rev. **B 47**, 11969 (1993).
- [19] P. Butera and M. Comi, Phys. Rev. **B 50**, 3052 (1994).
- [20] M. Campostrini, A. Pelissetto, P. Rossi and E. Vicari, Nucl. Phys. **B459**, 207 (1996).
- [21] D. L. Hunter and G. A. Baker Jr., Phys. Rev. **B 7**, 3346 (1972) and references therein.
- [22] A. J. Guttmann, “Phase Transitions and Critical Phenomena”, vol. 13, C. Domb and J. Lebowitz eds. (Academic Press, New York).
- [23] A. J. Guttmann and G. S. Joyce, J. Phys. **A5** L81 (1972); D. L. Hunter and G. A. Baker Jr., Phys. Rev. **B 49** 3808 (1979).
- [24] A. J. Guttmann, J. Phys. **A20**, 1839 (1987).
- [25] A. J. Guttmann, J. Phys. **A22**, 1989 (1989).
- [26] P. G. de Gennes, Phys. Lett. **38A**, 339 (1972).
- [27] V. Matveev and R. Shrock, hep-lat 9412076, J. Phys. **A**, in press.
- [28] T. T. Wu, B. M. McCoy, C. A. Tracy, and E. Baruch, Phys. Rev. **B13**, 316 (1976).

- [29] M. E. Fisher and R. J. Burford, Phys. Rev. **156**, 583 (1967).
- [30] H. Cheng and T. T. Wu, Phys. Rev. **164**, 719 (1967).
- [31] J. Stephenson, J. Math. Phys. **5**, 1009 (1964).

## FIGURES

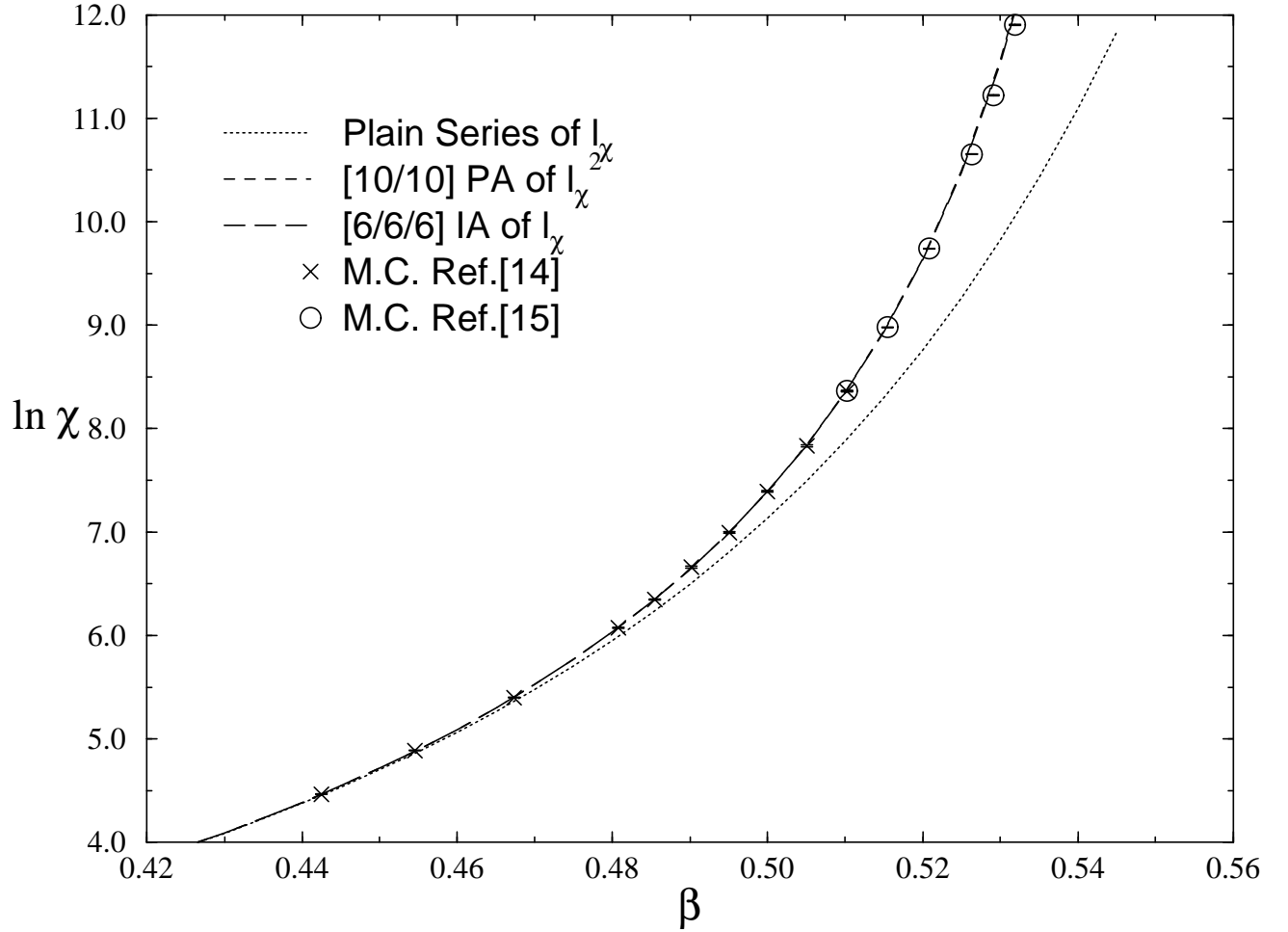


FIG. 1.  $\ln \chi$  vs.  $\beta$ . Beside Monte Carlo data from Refs. [14,15], we show curves constructed from the plain series of  $\ln \chi$ , from the [10/10] PA of  $l_\chi^2$ , and from the [6/6/6] IA of  $l_\chi$  biased at  $\beta_c = 0.5583$ , such that  $\sigma \simeq 0.50$ .

## TABLES

TABLE I. For various values of  $N < 2$  and for all lattices considered we report  $\beta_c^{(\chi)}$  and  $\gamma$  as obtained from a Dlog-PA analysis of the strong-coupling series of  $\chi$ , and  $\beta_c^{(\xi)}$  and  $\nu$  from that of  $\xi_G^2$ . Defective Dlog-PA's, i.e., those with spurious singularities close to the real axis for  $\text{Re}\beta \lesssim \beta_c$  (e.g.,  $\text{Re}\beta < 1.1\beta_c$ ) are discarded. An asterisk indicates that most of Dlog-PA's considered are defective and the estimate comes just from a few of them, or in the cases where numbers are not shown that all Dlog-PA's are defective, so that no estimate can be extracted.

| $N$             | lattice    | $\beta_c^{(\chi)}$ | $\gamma$   | $\beta_c^{(\xi)}$ | $\nu$       |
|-----------------|------------|--------------------|------------|-------------------|-------------|
| $-\frac{7}{4}$  | triangular | 0.1728(4)          | 1.04(2)    | *                 | *           |
|                 | Eq. (3)    |                    | 1.05371... |                   | 0.547925... |
| $-\frac{3}{2}$  | square     | 0.258(1)           | 0.80(3)    | 0.252(1)          | 0.65(5)     |
|                 | triangular | 0.1875(2)          | 1.09(1)    | 0.1888(4)         | 0.64(1)     |
|                 | honeycomb  | *0.339(1)          | *0.80(5)   | 0.3319(1)         | 0.52(1)     |
|                 | Eq. (3)    |                    | 1.08759... |                   | 0.574690... |
| $-1$            | square     | 0.3144(1)          | 1.13(1)    | *0.3141           | *0.60       |
|                 | triangular | 0.2082(1)          | 1.14(1)    | 0.2086(1)         | 0.642(3)    |
|                 | honeycomb  | 0.42332(5)         | 1.11(1)    | 0.4240(6)         | 0.64(4)     |
|                 | Eq. (3)    |                    | 1.15625    |                   | 0.625       |
| $-\frac{1}{2}$  | square     | 0.34919(6)         | 1.233(5)   | 0.34922(2)        | 0.681(1)    |
|                 | triangular | 0.2252(2)          | 1.23(2)    | 0.22528(2)        | 0.687(1)    |
|                 | honeycomb  | 0.48504(3)         | 1.233(3)   | 0.48498(2)        | 0.672(1)    |
|                 | Eq. (3)    |                    | 1.23758... |                   | 0.680715... |
| $0$             | square     | 0.37900(4)         | 1.334(2)   | 0.37905(2)        | 0.750(1)    |
|                 | triangular | 0.24087(4)         | 1.332(5)   | 0.24092(3)        | 0.750(2)    |
|                 | honeycomb  | 0.54117(3)         | 1.341(3)   | 0.54116(1)        | 0.748(1)    |
|                 | Eq. (3)    |                    | 1.34375    |                   | 0.75        |
| $\frac{1}{2}$   | square     | 0.40854(1)         | 1.494(1)   | 0.408530(3)       | 0.8453(2)   |
|                 | triangular | 0.25686(5)         | 1.484(4)   | 0.25692(1)        | 0.8450(1)   |
|                 | honeycomb  | 0.59730(2)         | 1.492(1)   | 0.59731(1)        | 0.8446(1)   |
|                 | Eq. (3)    |                    | 1.49641... |                   | 0.845852... |
| $1$             | square     | 0.440684(1)        | 1.7496(1)  | 0.440690(5)       | 1.0002(2)   |
|                 | triangular | 0.27466(1)         | 1.750(2)   | 0.27466(1)        | 1.0005(5)   |
|                 | honeycomb  | 0.65849(2)         | 1.750(1)   | 0.65846(2)        | 1.000(1)    |
|                 | Eq. (3)    |                    | 1.75       |                   | 1           |
| $\frac{3}{2}$   | square     | 0.4804(2)          | 2.30(1)    | 0.4802(2)         | 1.31(2)     |
|                 | triangular | 0.2967(1)          | 2.30(2)    | 0.2965(1)         | 1.31(1)     |
|                 | honeycomb  | 0.73371(8)         | 2.313(5)   | 0.7337(3)         | 1.33(1)     |
|                 | Eq. (3)    |                    | 2.31987... |                   | 1.33672...  |
| $\frac{7}{4}$   | square     | 0.5072(4)          | 2.97(5)    | 0.5066(4)         | 1.66(4)     |
|                 | triangular | 0.3114(2)          | 2.91(4)    | 0.3111(5)         | 1.65(9)     |
|                 | honeycomb  | 0.7844(5)          | 3.01(5)    | 0.7845(10)        | 1.74(9)     |
|                 | Eq. (3)    |                    | 3.12490... |                   | 1.80413...  |
| $\frac{19}{10}$ | square     | 0.529(1)           | 4.0(2)     | *                 | *           |
|                 | triangular | 0.3230(4)          | 3.7(1)     | 0.323(2)          | 2.2(3)      |
|                 | honeycomb  | 0.826(2)           | 4.0(2)     | 0.827(4)          | 2.4(3)      |
|                 | Eq. (3)    |                    | 4.72210... |                   | 2.72322...  |

TABLE II. First-order integral-approximant analysis of the 20th order strong-coupling series of  $l_\chi \equiv \beta^{-1} \ln \chi$  on the square lattice. Asterisks mark defective approximants, i.e., those having spurious singularities close to the real axis for  $\text{Re}\beta \lesssim \beta_c$ .

| $N$ | $m$ | $l$ | $k$ | $\beta_c$ | $\sigma$ |
|-----|-----|-----|-----|-----------|----------|
| 19  | 6   | 6   | 5   | 0.5598    | 0.55     |
|     | 6   | 5   | 6   | *         |          |
|     | 7   | 5   | 5   | 0.5563    | 0.42     |
| 20  | 6   | 6   | 6   | 0.5598    | 0.59     |
|     | 7   | 6   | 5   | 0.5585    | 0.51     |
|     | 7   | 5   | 6   | 0.5565    | 0.37     |

TABLE III. On the square lattice, IA analysis of the series  $\lambda_\chi$  constructed from the series of  $l_\chi$  and  $l_\chi^2$  according to CPRM.  $\sigma_{\text{biased}}$  is obtained by biasing  $x_c = 1$ .

| $N$ | $m$ | $l$ | $k$ | $x_c$  | $\sigma$ | $\sigma_{\text{biased}}$ |
|-----|-----|-----|-----|--------|----------|--------------------------|
| 18  | 6   | 5   | 5   | *      |          | 0.522                    |
| 19  | 5   | 6   | 6   | 1.0082 | 0.64     | 0.509                    |
|     | 6   | 6   | 5   | 1.0026 | 0.55     | 0.485                    |
|     | 6   | 5   | 6   | *      |          | 0.536                    |
| 20  | 6   | 6   | 6   | 1.0042 | 0.57     | *                        |
|     | 6   | 7   | 5   | 1.0043 | 0.59     | 0.506                    |
|     | 6   | 5   | 7   | 1.0198 | 1.05     | 0.501                    |
|     | 7   | 6   | 5   | 1.0039 | 0.58     | 0.523                    |
|     | 7   | 5   | 6   | 1.0035 | 0.59     | 0.467                    |

TABLE IV. On the triangular lattice, analysis of the series  $\lambda_\chi$  constructed from the series of  $l_\chi$  and  $l_\chi^2$  according to CPRM.  $\sigma_{\text{biased}}$  is obtained by biasing  $x_c = 1$ . We noted here that sometime biasing the singularity at  $x_c = 1$  gives rise to spurious singularities in the real axis for  $x_c \lesssim 1$ . We considered approximants with singularities in the region  $[0.8, 1.2]$  defective, and they are marked by an asterisk. In these cases the estimate of the exponent from non-biased approximants should be more reliable.

| $N$ | $m$ | $l$ | $k$ | $x_c$  | $\sigma$ | $\sigma_{\text{biased}}$ |
|-----|-----|-----|-----|--------|----------|--------------------------|
| 11  | 3   | 3   | 3   | 0.9723 | 0.192    | 0.501                    |
| 12  | 3   | 3   | 4   | 0.9808 | 0.258    | 0.504                    |
|     | 3   | 4   | 3   | 0.9881 | 0.335    | 0.503                    |
|     | 4   | 3   | 3   | 0.9992 | 0.490    | 0.502                    |
| 13  | 3   | 4   | 4   | 0.9954 | 0.446    | 0.510                    |
|     | 4   | 3   | 4   | 1.0017 | 0.534    | 0.518                    |
|     | 4   | 4   | 3   | 1.0027 | 0.549    | *                        |
|     | 5   | 3   | 3   | 1.0026 | 0.541    | 0.493                    |
| 14  | 4   | 4   | 4   | 1.0016 | 0.532    | 0.550                    |
|     | 4   | 5   | 3   | 1.0003 | 0.484    | 0.477                    |
|     | 4   | 3   | 5   | 1.0015 | 0.533    | 0.485                    |
|     | 5   | 3   | 4   | 1.0015 | 0.533    | *                        |
|     | 5   | 4   | 3   | 1.0021 | 0.520    | 0.520                    |
|     | 6   | 3   | 3   | 1.0016 | 0.523    | 0.481                    |

TABLE V. The strong-coupling estimates of  $\xi_G$  are compared with some available Monte Carlo results on the square lattice, taken from Ref. [14] and obtained by standard Monte Carlo, and Ref. [15] by finite-size scaling techniques. The strong-coupling estimates of  $\xi_G$ ,  $\xi_G^{(1)}$  and  $\xi_G^{(2)}$ , are obtained respectively from [9/9],[10/9],[9,10],[8/11] PA's of  $l_\xi^2$ , and from [5/6/6], [6/6/5], [6/5/6], [5/6/5], [5/5/6], [6/5/5] IA's of  $l_\xi$  biased at  $\beta_c = 0.559$ . We again warn that the errors displayed in the strong-coupling estimates are related to the spread of the different approximants considered. The asterisk indicates that the number concerns  $\xi_{\text{exp}}$ , and not  $\xi_G$ .

| $\beta$ | $\xi_G^{(1)}$ | $\xi_G^{(2)}$ | $\xi_G^{(\text{MC})}$ [14] | $\xi_G^{(\text{FSS})}$ [15] |
|---------|---------------|---------------|----------------------------|-----------------------------|
| 1/2.2   | 9.320(3)      | 9.318(1)      | 9.32(2)*                   |                             |
| 1/2.08  | 18.76(3)      | 18.74(1)      | 18.75(6)                   |                             |
| 1/2.04  | 26.3(1)       | 26.21(2)      | 26.4(2)*                   |                             |
| 0.5     | 40.3(3)       | 40.08(6)      | 40.4(4)*                   |                             |
| 1/1.98  | 52.2(3)       | 52.0(1)       | 51.3(9)*                   |                             |
| 1/1.96  | 70.8(7)       | 70.3(2)       | 69.9(8)                    | 70.4(4)                     |
| 1/1.94  | 102(2)        | 100.7(5)      |                            | 100.3(7)                    |
| 1/1.92  | 158(3)        | 156(1)        |                            | 156(2)                      |
| 1/1.90  | 276(11)       | 269(3)        |                            | 263(3)                      |
| 1/1.88  | 570(30)       | 549(10)       |                            | 539(5)                      |
| 1/1.87  | 910(60)       | 860(20)       |                            | 847(7)                      |

TABLE VI. Summary of the determinations of  $\beta_c$  and  $\sigma$  on the square, triangular and honeycomb lattices by different analysis. A bias in the analysis is indicated by a subscript in the corresponding abbreviation.

| lattice    | series         | analysis             | $\beta_c$  | $\sigma$ |
|------------|----------------|----------------------|------------|----------|
| square     | $l_\chi$       | DLPA                 | 0.560(2)   | 0.53(4)  |
|            | $l_\chi$       | IA                   | 0.558(2)   | 0.49(8)  |
|            | $\lambda_\chi$ | CPRM-DLPA $_{x_c=1}$ |            | 0.51(4)  |
|            | $\lambda_\chi$ | CPRM-IA $_{x_c=1}$   |            | 0.50(2)  |
|            | $\lambda_\xi$  | CPRM-IA $_{x_c=1}$   |            | 0.59(6)  |
|            | $l_\chi^2$     | PA                   | 0.5579(3)  |          |
|            | $l_\chi^2$     | IA $_{\sigma=1/2}$   | 0.5583(2)  |          |
|            | $l_\xi^2$      | PA                   | 0.558(1)   |          |
| triangular | $l_\chi$       | IA $_{\sigma=1/2}$   | 0.559(1)   |          |
|            | $l_\chi$       | DLPA                 | 0.3413(3)  | 0.52(2)  |
|            | $l_\chi$       | IA                   | 0.33986(4) | 0.473(3) |
|            | $\lambda_\chi$ | CPRM-DLPA $_{x_c=1}$ |            | 0.53(1)  |
|            | $\lambda_\chi$ | CPRM-IA $_{x_c=1}$   |            | 0.50(2)  |
|            | $\lambda_\xi$  | CPRM-IA $_{x_c=1}$   |            | 0.52(4)  |
|            | $l_\chi^2$     | PA                   | 0.3400(2)  |          |
|            | $l_\xi^2$      | PA                   | 0.3393(1)  |          |
| honeycomb  | $l_\chi$       | IA $_{\sigma=1/2}$   | 0.3410(5)  |          |
|            | $l_\chi$       | DLPA                 | 0.884(1)   | 0.54(1)  |
|            | $l_\chi$       | IA                   | 0.877(6)   | 0.4(2)   |
|            | $l_\chi^2$     | PA                   | 0.879(1)   |          |
|            | $l_\chi^2$     | IA $_{\sigma=1/2}$   | 0.880(1)   |          |
|            | $l_\xi^2$      | PA                   | 0.878(2)   |          |
|            | $l_\xi^2$      | IA $_{\sigma=1/2}$   | 0.883(1)   |          |

TABLE VII. We report  $s^*$ ,  $c_2$  and  $c_3$  as obtained from the analysis of the strong-coupling series in  $\beta$  (first line) and in  $E$  (second line) on the square, triangular and honeycomb lattices. Beside the spread of estimates from different PA's and Dlog-PA's, the errors displayed take also into account the uncertainty on  $\beta_c$  and  $E_c$ . We do not report the estimates of  $c_3$  by the analysis of the  $\beta$ -series because their uncertainty is much larger than those from the  $E$ -series.

| lattice    | $\beta_c, E_c$         | $s^*$      | $c_2$      | $c_3$      |
|------------|------------------------|------------|------------|------------|
| square     | $\beta_c \simeq 0.559$ | 0.9985(12) | 0.000(2)   |            |
|            | $E_c \simeq 0.722$     | 0.9984(7)  | -0.0014(3) | 0.00001(2) |
| triangular | $\beta_c \simeq 0.340$ | 0.9979(11) | -0.002(2)  |            |
|            | $E_c \simeq 0.68$      | 0.9985(11) | -0.0010(3) | 0.00001(5) |
| honeycomb  | $\beta_c \simeq 0.880$ | 0.9988(10) | -0.001(3)  |            |
|            | $E_c \simeq 0.77$      | 0.9987(5)  | -0.0021(4) | 0.00003(2) |

TABLE VIII. For  $N = 1$  and  $N = 0$  we report  $s^*$ ,  $c_2$  and  $c_3$  as obtained from the analysis of the available strong-coupling series in  $\beta$  on the square, triangular and honeycomb lattices. The analyses of the corresponding energy series provide consistent but less precise results, so we do not report their results.

|     | lattice    | $\beta_c$                                       | $s^*$      | $c_2$       | $c_3$       |
|-----|------------|---|------------|-------------|-------------|
| N=1 | square     | $\frac{1}{2} \ln(\sqrt{2} + 1) = 0.440687\dots$ | 0.99909(2) | -0.00094(3) | 0.000008(5) |
|     | triangular | $\frac{1}{4} \ln 3 = 0.274653\dots$             | 0.99912(5) | -0.00098(4) | 0.00001(1)  |
|     | honeycomb  | $\frac{1}{2} \ln(2 + \sqrt{3}) = 0.658478\dots$ | 0.99907(2) | -0.00093(3) | 0.000012(2) |
| N=0 | square     | 0.3790527(2) [24]                               | 1.0001(2)  | 0.00016(8)  | 0.00000(1)  |
|     | triangular | 0.240920(1) [24]                                | 1.0002(4)  | 0.0003(5)   | 0.00000(3)  |
|     | honeycomb  | $(2 + \sqrt{2})^{-1/2} = 0.541196\dots$ [9]     | 0.9998(2)  | 0.00010(7)  | -0.00002(1) |